

THESIS

IMPACTS OF DROUGHT ON GRASSLAND PRODUCTIVITY ACROSS THE
WET-DRY GRADIENT IN THE U.S. GREAT PLAINS IN 2010-2012

Submitted by

Renee A. Curry

Graduate Degree Program in Ecology

In partial fulfillment of the requirements

For the Degree of Master of Science

Colorado State University

Fort Collins, Colorado

Fall 2016

Master's Committee:

Advisor: A. Scott Denning

Melinda Smith

Lori Peek

Copyright by Renee Ann Curry 2016

All Rights Reserved

ABSTRACT

IMPACTS OF DROUGHT ON GRASSLAND PRODUCTIVITY ACROSS THE WET-DRY GRADIENT IN THE U.S. GREAT PLAINS IN 2010-2012

Severe, prolonged droughts are predicted to occur more frequently due to global climate change. Since grasslands already grow in regions that are water limited, they are particularly vulnerable to changes in precipitation. Climate models are used to investigate how grasslands will respond to climate change; however, current land surface models have difficulty in simulating grasslands and their response to drought. The main objective of this research project was to investigate the dominant relationships between grassland productivity and precipitation and to see if this behavior could be predicted in a model. To do this, we focused on both climate (dry to wet gradient) and drought (climate anomalies) using a combination of data and the Simple Biosphere Model Version 4 (SiB4). In order to have a better understanding of the relationship between grassland productivity and precipitation on a regional scale, this research studies nine sites across the U.S. Great Plains over which there is a significant precipitation gradient. In addition to the climatic gradient in precipitation, we took advantage of a natural experiment from 2010 through 2012, during which a significant drought occurred in this region.

Observed west-to-east gradients in grassland productivity were generally well-captured by the model: there was an increase in leaf area index (LAI) with increasing precipitation, with a nearly identical linear relationship in both the observations and the model. SiB4 overestimated the magnitude of the seasonal-mean LAI; however, this bias was constant across the precipitation gradient. The drought decreased grassland productivity: both the observations and the model

showed reduced LAI and a shorter growing season due to drought, and an analysis of the standardized anomalies in LAI and precipitation demonstrated that both the observations and the model have a nearly identical linear response to drought (difference in slope $< 10\%$). Although SiB4 has a bias in the magnitude of seasonal-mean LAI, it has the same precipitation responses as seen in the data, thus showing the ability to capture the behavior of grasslands both across a dry-wet gradient and for a specific drought event.

ACKNOWLEDGEMENTS

I am extremely grateful for the guidance and mentoring from my advisor, Dr. A. Scott Denning. Additionally, I would like to thank my committee members, Dr. Melinda Smith and Dr. Lori Peek. Thank you to Dr. Smith for her additional insight on grassland ecology and the Konza Prairie Research Station. Thank you to Marcy Litvak for her discussions on the Sevilleta National Wildlife Refuge Research Station.

Many thanks to my colleague, Dr. Kathy Haynes, for all of her help in learning about this new model and beyond. This project could not have been completed without her help and her friendship. Thank you to Matt Bishop and Ammon Redman for all of their computing help. I also want to thank all of my wonderful Biocycle group members for their guidance and friendship especially Ian Baker and Nick Geyer. Thank you to Dr. Justin Derner and David Augustine from the local USDA-ARS for their help on the new grazing component in the model and additional information the Shortgrass Steppe research site.

I want to thank my friends, mentors, and family for their continuous support during the completion of this degree. Lastly, I would especially like to thank my new husband, Jay Minaya, and his wonderful family for their unconditional love and support. I am so grateful to my husband for his patience, understanding and support in regards to my career.

The MODIS LAI subset data used in this study was acquired from NASA's Oak Ridge National Laboratory Distributed Active Archive Center for Biogeochemical Dynamics (ORNL DAAC). This work used eddy covariance data acquired by the FLUXNET community and in particular by the following networks: AmeriFlux (U.S. Department of Energy, Biological and Environmental Research, Terrestrial Carbon Program (DE-FG02-04ER63917 and DE-FG02-

04ER63911)), AfriFlux, AsiaFlux, CarboAfrica, CarboEuropeIP, CarboItaly, CarboMont, ChinaFlux, Fluxnet-Canada (supported by CFCAS, NSERC, BIOCAP, Environment Canada, and NRCan), GreenGrass, KoFlux, LBA, NECC, OzFlux, TCOS-Siberia, USCCC. We acknowledge the financial support to the eddy covariance data harmonization provided by CarboEuropeIP, FAO-GTOS-TCO, iLEAPS, Max Planck Institute for Biogeochemistry, National Science Foundation, University of Tuscia, Université Laval and Environment Canada and US Department of Energy and the database development and technical support from Berkeley Water Center, Lawrence Berkeley National Laboratory, Microsoft Research eScience, Oak Ridge National Laboratory, University of California - Berkeley, and University of Virginia.

This research was supported by the National Science Foundation Science and Technology Center for Multi-Scale Modeling of Atmospheric Processes, managed by Colorado State University under cooperative agreement No.ATM-0425247.

TABLE OF CONTENTS

| | |
|--|----|
| Abstract | ii |
| Acknowledgements | iv |
| 1. Introduction | 1 |
| 1.1 Land Surface Models and Grasslands | 1 |
| 1.2 Climate Change and Drought | 3 |
| 1.3 Natural Experiments | 6 |
| 1.3.1 Climatological West-East Gradient | 6 |
| 1.3.2 2010-2012 Drought | 9 |
| 2. Methods | 13 |
| 2.1 MODIS Leaf Area Index | 13 |
| 2.2 Eddy Covariance/Flux Tower Data | 14 |
| 2.3 Seasonal Mean LAI and Water Deficit Calculations | 16 |
| 2.4 Simple Biosphere Model Version 4 (SiB4) Background | 17 |
| 3. Results and Discussion | 22 |
| 3.1 Climatological Wet-Dry Gradient | 22 |
| 3.2 Seasonality | 24 |
| 3.2.1 Leaf Area Index (LAI) | 24 |
| 3.2.2 Energy and Carbon Fluxes | 28 |
| 3.3 Interannual Variability | 32 |
| 4. Conclusion | 35 |
| 5. Future Work | 38 |
| Tables and Figures | 40 |
| References | 73 |

CHAPTER 1: INTRODUCTION

1.1 Land Surface Models and Grasslands

Climate predictions are important in order to understand how ecosystems will respond to the increasing levels of CO₂. Due to the increase in CO₂, there has been and will continue to be an increase in global temperatures. Predictions have indicated that extreme events such as drought will be more commonplace with the changing climate (IPCC 2013). Droughts can significantly reduce ecosystem productivity; however, the effects of drought may be buffered by the CO₂ fertilization effect, as both plant productivity and water use efficiency increase with the increase in atmospheric CO₂ concentrations (Moran et al., 2014; Donohue et al., 2013; Swann et al. 2016). Drought reduces the productivity of grasslands and crops, which impacts stakeholders. Climate models have some skill in predicting these drought impacts on productivity, but many “impacts” models driven by climate model output do not include the effect of CO₂ on water use efficiency and therefore substantially overestimate drought impacts (Swann et al., 2016).

Terrestrial biosphere models (TBMs) incorporate the main processes influencing vegetation to provide analysis of the land surface interactions. These TBMs are incorporated into the global climate models that perform climate predictions. While TBMs are essential in climate prediction, grasslands in particular have been one of the hardest vegetation types for TBMs to model accurately. Recently, the North American Carbon Program (NACP) organized several synthesis activities to evaluate and inter-compare TBMs (Huntzinger et al., 2013). Three studies have analyzed the performance of TBMs, including specific grassland evaluations. First, a paper from Schwalm et al. (2010) compared observed and modeled monthly carbon fluxes from 44 flux tower sites and 22 terrestrial biosphere models. This study included over 220 site-

years, 10 biomes, and two significant droughts. After evaluating modeled seasonal cycles of CO₂ exchange using numerous metrics, they concluded that overall model performance was poor. They found that the models performed better at capturing the gross fluxes in forested sites compared to unforested sites, such as grasslands.

Next, a study by Schaefer et al. (2012) used 29 models and 39 flux towers to evaluate model prediction of GPP. This study found that none of the models matched estimated GPP within observed uncertainty; however, it did show that the models estimated the GPP more accurately at forest sites than at crop, grass and savanna sites. Overall, the models overestimated the gross fluxes of grassland sites during the growing season, which could be the result of the model's lack of ability to accurately determine the stresses due to soil moisture, drought and humidity stress (Schaefer et al. 2012).

Finally, Razcka et al. (2013) compared 17 models against 36 flux tower sites in North America over a five-year timeframe to determine how well TBM models predict carbon and energy fluxes. The models performed the best at deciduous broadleaf forest sites and the worst at crop, evergreen and grassland sites. For grasslands, there were biases of 66% in net ecosystem exchange (NEE), 41% in gross primary productivity (GPP) and 61% in total respiration (RE). In regards to seasonal variability, modeled fluxes for crop and grassland sites performed the most poorly when comparing the model to observations. Although the study concludes that these models better simulated the seasonality than the inter-annual variability, for grasslands the TBMs had a lag in the start of the growing season and the growing season length was two or three months too long. All of these examples illustrate the need to improve the TBM's prediction of carbon and energy fluxes in grasslands. The significant seasonal discrepancies and poor skill at capturing inter-annual variability indicate that grasslands need substantial improvement in

TBMs. Being capable of predicting inter-annual variability is a key step to accurately predicting drought, one of the most influential disturbances in grassland regions.

Grasslands are driven by disturbances such as fire, grazing and drought. Grasses have evolved unique morphology, development patterns and physiology over time to best adapt to these disturbances. However, grasslands are still sensitive to short-term climate variability and long-term climate change. Many areas of the U.S. Great Plains are susceptible to drought because the annual water loss combined from transpiration by plants and from evaporation is higher than the annual precipitation. The trend of climate projections of the U.S. Great Plains indicate that there will be more dry days and higher temperatures that will lead to an increase in evapotranspiration and a decrease in water resources (Blair et al., 2014). Climate change, especially in conjunction with increased grazing pressure, is expected to have long-term impacts on sustainability of grassland ecosystems including a decrease in species habitat for permanent and migrating species (Bagne et al., 2012). Thus, it is essential that we improve our understanding of how grasslands in the U.S. Great Plains will respond to the changing climate and drought.

1.2 Climate Change and Drought

These terrestrial biosphere models are important in predicting the impacts of climate change. The global climate is changing and this change is apparent across a wide range of observations. According the National Climate Assessment, the average temperature in the United States has increased by about 0.7°C to 1.0°C since 1895, but most of the increase has occurred since 1970. The recent decade was the warmest on record for the U.S, and temperatures in the U.S. and other locations around the world are expected to continue to increase (Walsh et al.,

2014; IPCC 2013). Figure 1 illustrates the projected temperature change for the U.S. in the later part of this century relative to the later part of the last century under a low and high emission scenario. As a worst case, the temperatures increase at least 3.3°C (6°F) for the entire U.S., with the majority of the contiguous U.S. increasing approximately 4.44°C (8°F). Even with a drastic reduction in emissions from the current rate, temperatures still increase from about 1.7°C (3°F) to 2.78°C (5°F.) Due to warming, the length of the growing season has been increasing since the 1980s and is expected to keep increasing (Kunkel 2016).

In regards to the response of precipitation to climate change, the difference between wet and dry areas will increase both in the U.S. and globally: wet areas will get wetter while dry areas will get drier (IPCC 2013; Walsh et al., 2014; Shafer et al., 2014). In addition, certain types of extreme weather events with links to climate change have become and will continue to be more frequent and/or intense, including prolonged periods of heat, heavy downpours, and, in some regions, floods and droughts (IPCC 2013; Walsh et al. 2014). Days considered to be “hot days” are expected to increase in number over the U.S. especially by the late century. Heat waves have already occurred more frequently and have become more intense in the recent decade. The Southwest and Central regions of the U.S. are projected to have more frequent and more intense heat waves in the summer (Melilo et al., 2014; Shafer et al., 2014). Under higher emissions scenarios, widespread drought is projected to become more commonplace over most of the central and southern United States (Melilo et al., 2014; Walsh et al., 2014).

Changes in precipitation and temperature create feedbacks that further impact the climate. Figure 2 illustrates projected changes in water balance due to climate change from the Intergovernmental Panel on Climate Change Fifth Assessment Report (IPCC AR5) using a high emission scenario (RCP 8.5) for 2081-2100 relative to 1986-2005 (Stocker et al., 2013).

Changes in precipitation over the U.S Great Plains (center of black circle) are indeterminate, but increases in evaporation due to warmer temperatures are robust, even accounting for increased water use efficiency due to higher CO₂. As a result, projected soil moisture shows a significant decrease of around 10% for the southwest portion of the domain which means that there will be additional drought stress. The projected increase in temperature results in increased evaporation, decreased soil moisture, additional heat stress and, therefore, higher energy demand for cooling. Even in areas where the precipitation does not decrease, the increase of the loss of moisture through the leaves of water loss from plants can lead to soils drying out at a quicker rate, which in turn leads to hotter summers under drier climatic conditions. In addition, the ecosystem water balance might change overall due to the change in rainfall and the carbon sinks might offset some of the carbon emissions (Walsh et al., 2014, Shafer et al., 2014; Swann et al., 2016).

These impacts on climate will affect ecosystems both positively and negatively (Bagne et al., 2012). For grasslands across the U.S., the regions suitable for these ecosystems is expected to increase; however, projections vary by grassland type. In addition to changing the areal coverage, climate change will also have an impact on grassland species and community composition. While grasslands will be significantly affected by climate change, complex interactions make grassland predictions difficult, and there is still uncertainty in regards to how grasslands will respond to the longer, warmer droughts and more intense rainfall events that are expected with the changing climate (Moran et al., 2014).

In addition to impacting vegetation and grasslands, droughts stress the natural resources and increase the competition of water demand on a variety of stakeholders. There are a variety of significant economic, social and environmental stresses that can worsen or improve drought. This flow chart (Figure 3) focuses on the drought impacts to agricultural and non-

agricultural sectors and the negative impacts on end-users, such as farmers, ranchers, tourists and municipal water utilities (Kellner & Niyogi 2014). Existing adaptation and planning efforts are inadequate to respond to these projected impacts (Parry et al., 2007; Walsh et al., 2014).

1.3 Natural Experiments

1.3.1 Climatological West-East Gradient

The Great Plains is a vast grassland region in the central U.S. that ranges from the flat plains near sea level to elevations above 1500 meters near mountainous regions. In addition to the changes in elevation, the annual average precipitation and temperature changes significantly across the U.S. Great Plains. The region has a considerable north-south gradient in the annual average temperature that ranges from less than 4°C in the mountains of Wyoming and Montana to higher than 20°C in South Texas (Figure 4). Annual average precipitation is greater than 1270 millimeters (50 inches) in the tall-grass prairies in the eastern part of this domain; however, in the majority of the domain, the average precipitation is less than 760 millimeters, with annual rainfall of less than 300 millimeters along the western edges of the domain (desert grassland in New Mexico), as shown in Figure 5 (PRISM).

Given this variability in temperature and precipitation in the region of the U.S. Great Plains as shown in Figures 4 and 5, grasslands vary from the semi-arid short grass steppe in the west, the northern mixed prairie, the southern mixed prairie and the sub-humid tall-grass prairie in the east. Temperate, perennial grassland ecosystems in the U.S. Great Plains receive the most of their annual precipitation during the growing season and then the grasslands go into dormancy in order to survive the cold winter temperatures.

The grasslands in this region are composed of C₃ and C₄ plant functional types (PFTs). These two PFTs have important and distinct functionalities in water cycling and productivity. C₃ grasses tend to grow in the cool-wet season primarily found in the higher latitudes or higher elevations (Teeri & Stowe, 1976; Paruelo & Lauenroth, 1996; Tieszen et al., 1997; Davidson & Csilag, 2003; Winslow et al., 2003; Still et al., 2003). C₃ grasses usually begin growing early in the spring and may have a secondary peak in autumn. In contrast, C₄ grasses are warm-season grasses that start growing later and in warmer environments compared to C₃ grasses. Due to the difference in photosynthetic pathways, C₄ has growth advantages in areas with higher sunlight and higher temperatures.

The C₃ and C₄ grassland PFTs grow in mixed compositions in the U.S. Great Plains and their relative abundance changes due to the weather conditions each year. It is well known from observations that C₃ and C₄ grasses partition along moisture and temperature gradients such as in the Great Plains (Chazdon 1978; Vogel et al., 1986). Since C₄ grasses have a higher tolerance for higher temperatures compared to C₃, C₄ species are more dominant in the south, while shortgrass C₃ species are found mostly in the northern part of this domain. C₃ and C₄ plants can co-exist but C₄ plants will be more competitive and thus more abundant in grassland regions where the mean monthly air temperature exceeds 22 °C (Collatz et al., 1998; Still et al., 2003).

Drought tolerance is also important in this C₃/C₄ distribution due to the differences in photosynthetic pathways. Generally C₄ species are more drought tolerant than C₃ species because these grasses are more efficient at photosynthesis. Since C₄ grasses eliminate photorespiration, C₄ plants are much less limited by CO₂ and have a higher water use efficiency (Taylor et al., 2010; Still et al., 2003). In addition to being more efficient at photosynthesis, the

production of deep roots in C4 grasses has long been discussed as a mechanism to avoid drought (Albertson and Weaver 1944; Weaver 1968; Craine et al., 2002; Nippert et al., 2011). Although the root systems of grasslands are highly variable in terms of species-specific patterns, total biomass invested, types of roots produced, and distribution throughout the soil profile, in general C4 grasses typically have fewer roots that grow to a deeper depth than C3 grasses (Blair et al. 2014). While the majority of grassland root biomass is found in the upper layers of the soil, during drought these deep roots help the grasses mitigate the impacts of drought. It is important to note that C3 and C4 grasses have different root characteristics but that is not represented in the current TBMs.

The U.S. Great Plains provides a natural experiment to investigate the response of grassland productivity to different precipitation amounts across a large climatological gradient. Grasslands are well-known for growing under a broad range of climatic conditions, and they are more responsive to variations in rainfall compared to other biomes or plant functional types (Sala et al., 2000, Knapp and Smith 2001, Suttle et al., 2007, Reichmann et al., 2013, Moran et al., 2014). Grasslands frequently experience high intra- and inter-annual rainfall variability, making both the seasonality (timing) and total annual amount of precipitation critical for these ecosystems (Craine et al., 2012). Thus, for any given location, grasses are highly responsive to variations in precipitation (Hsu et al., 2012, Knapp et al., 2015).

Studies of grassland productivity across the U.S. climatological gradient show a linear relationship between aboveground net primary production (ANPP) and annual precipitation (Paruelo et al. 1999; Knapp and Smith 2001; Moran et al., 2014). The linear relationship between ANPP and annual precipitation breaks down during very wet conditions, when ecosystems are no longer water limited (Knapp and Smith, 2001). Some recent results also

indicate that this linearity breaks down for extreme dry conditions (drought) in addition to extreme wet conditions; the linearity breaks at both of the extreme ends of precipitation (M. Smith, personal communication). In addition to depending on precipitation, grasslands are also influenced by temperature, and thus for global grasslands the ratio of the precipitation to the potential evapotranspiration (PET) is usually a better predictor of the ecological properties and process rates rather than just annual precipitation (Blair et al., 2014).

Given this previous work, this study will investigate if this linearity between LAI and precipitation breaks in both the real world and in SiB4 during the droughts of 2011- 2012 in the U.S. Great Plains.

1.3.2 2010-2012 Drought

The U.S. Great Plains provided another natural experiment to investigate the response of a variety of grasslands to significant drought from 2010-2012. A drought began in late 2010 (Figure 6) due to a strong La Niña that brought below average rainfall to the southern United States. Figures 6-14 from the National Drought Mitigation Center (NDMC) show the progression of the drought across the Great Plains. In 2011 the drought was primarily located in the Southern Great Plains. By the end of spring, the drought expanded from Texas to impact seven states in the South, with 21 percent of the country in moderate to exceptional drought (NCDC 2012). In terms of the temperature and precipitation data, the drought intensity peaked in the late summer and autumn of 2011, and was the most intense drought on record for Texas (Figures 7-10). This region was so hot and dry that it took until the spring of 2015 for this area to fully recover.

The summer 2011 heat wave and drought in Texas was primarily driven by precipitation deficits (Walsh et al., 2014). According to the National Climatic Data Center (NCDC 2012), drought and heat wave conditions created major impacts across Texas, Oklahoma, New Mexico, Arizona, southern Kansas, and western Louisiana. In Texas and Oklahoma, a majority of range and pastures were classified in "very poor" condition for much of the 2011 main crop growing season. Most of these states mentioned broke the record for the highest monthly average temperature and hottest summer on record. The 2010-2011 drought resulted in a loss of over \$12 billion dollars and related to 95 deaths (NCEI 2016).

While the 2010 and 2011 drought are considered to be the same drought, the significant 2012 drought was considered a "flash" drought (not a continuation from 2011) and was located in the northern and eastern part of the Great Plains (Figures 11-14). The 2012 drought was a discrete event that developed suddenly and the official seasonal forecasts issued in April 2012 did not predict this severe, widespread drought. The 2012 drought occurred mainly due to the lack of atmospheric moisture in the spring from the Gulf of Mexico that usually provides the water vapor for the region (Hoerling et al., 2013). The below-average precipitation total stretched from the Intermountain West through the Great Plains into the Midwest and Southeast. Nebraska and Wyoming had record dry conditions in 2012.

The summer temperatures of 2012 ranked in the hottest 10% of the 118-year period of record in 28 states covering the Rocky Mountain states, the Great Plains, the Upper Midwest, and the Northeast (NCDC 2013). The 2012 drought is the most extensive drought to affect the U.S. since the 1930s. Moderate to extreme drought conditions affected more than half the country for a majority of 2012. According to NCDC (2013), the drought severely impacted the agriculture in the center of the country involving a widespread failure in harvest for the main

crops of corn, soybeans and others. Wheat was not largely impacted given the timing of the significant drought conditions. Overall, this 2012 cost over \$31 billion dollars and related to 123 deaths. In addition, the droughts of 2011 and 2012 led ranchers to liquidate large herds due to lack of food and water (USDA-ERS 2013; NCEI 2016).

The main objective of this research project was to investigate the dominant relationships between grassland productivity and precipitation and to see if this behavior could be predicted in a model. To do this, we focused on both climate (dry to wet gradient) and drought (climate anomalies) using a combination of data and the Simple Biosphere Model Version 4 (SiB4). The intention is to use the data to determine the grassland behavior and to use SiB4 to see if these processes can be captured and simulated in a model. To do this, we analyze remotely-sensed leaf area index (LAI), fluxes of carbon (net ecosystem exchange and gross primary production), and exchanges of energy (latent and sensible heat). In order to have a better understanding of the relationship between grasslands and precipitation on a regional scale, this research studies nine sites across the U.S. Great Plains (Figure 15; Table 1), over which there is a significant precipitation gradient (Figure 5). In addition to the climatic gradient in precipitation, we focus on the time period from 2010 through 2012, during which a significant drought occurred in this region (Figures 6-15).

There are three main questions that will be addressed in this study:

- 1) Over the 15-year MODIS record at the nine sites across the dry-to-wet gradient, is the seasonal mean LAI linear with respect to annual mean precipitation?
- 2) During the 2012 drought, do reductions in the seasonal mean LAI in response to large decrease in precipitation fall on the same line as the average response of LAI to climatological precipitation addressed in the first question?

- 3) Does the model capture these relationships as in the observations addressed in the first two questions?

For an outline of the rest of this paper, Chapter 2 will detail the methods, including the data used from both MODIS and FLUXNET, calculations and metrics used in this study, and the descriptions of SiB4. Chapter 3 focuses on the results and discussion of the climatological wet-dry gradient of the U.S. Great Plains, the seasonality of grassland LAI to precipitation and then the interannual variability including periods of drought from 2010-2012. Chapters 4 and 5 discuss the main conclusions and ideas for future work.

CHAPTER 2: METHODS

2.1 MODIS Leaf Area Index

Changes in aboveground live carbon pools over this three-year time period at various grassland sites (Table 1 and Figure 15) were analyzed by comparing simulated leaf area index (LAI) from SiB4 to Moderate Resolution Imaging Spectroradiometer (MODIS) data from the Terra and Aqua NASA satellites.

The Terra MODIS products are available with an acquisition date starting in February 2000, while Aqua are available starting in June 2002. The MODIS data were downloaded from the MODIS Land Product Subset website (<https://daac.ornl.gov/MODIS/>) data created by the Oak Ridge Laboratory Distributed Active Archive Center (ORNL DAAC 2008). The goal of the MODIS Subsets for Selected Field Sites is to prepare summaries of selected MODIS Land Products for the community to use for validation of models and remote sensing products and to characterize field sites.

MODIS FPAR is the Fraction of Absorbed Photosynthetically Active radiation that a plant canopy absorbs for photosynthesis and growth in the 0.4 – 0.7 nanometer (nm) spectral range. Leaf Area Index is the biomass equivalent of FPAR, and is also a dimensionless ratio (m^2/m^2) of leaf area covering a unit of ground area. We used the quality control flags given in the MODIS subset product in an intermediate level to smooth the noise out but not harsh enough to lose too much data (ORNL DAAC 2008).

MODIS is the best available dataset to compare to the values of the LAI from SiB4. However, there are some key differences. MODIS has a different timescale and larger footprint than SiB4. MODIS LAI values are based on an 8-day composite while SiB4 calculates LAI on a

daily time-step. In general, an 8-day MODIS composite represents the best value for that pixel considering all 8 days so that adjacent pixels with the same 8-day date may represent values from different overpasses. In addition, the 7x7 km grid cell of this MODIS product is larger than the single SiB4 pixel where the flux tower is/was located. Finally, this particular study only focuses on the grassland plant functional types (PFTs); however, the MODIS LAI values include all PFTs (ex. forests, crops) within that 7km by 7 km grid cell.

The nine sites were chosen (Table 1 and Figure 15) for this study from more than 1000 sites in this MODIS subset database. Our first selection criterion required that the MODIS subset data that was/currently co-located with a flux tower located in the region where the drought occurred from 2010-2012 in the U.S. Great Plains. The second criterion was the site had to be the grassland vegetation type as opposed to other types such as crops, forest, shrubland, juniper, etc. One additional site (Randall's Ranch) fit these criteria but was omitted due to its close proximity to another site in eastern Kansas, the Konza Prairie site.

2.2 Eddy Covariance/Flux Tower Data

The FLUXNET (flux tower) data, which is available at NASA's ORNL DAAC (Distributed Active Archive Center), was downloaded from the website: <http://fluxnet.ornl.gov/>. FLUXNET is a "network of regional networks," and coordinates regional and global analysis of observations from micrometeorological tower sites. FLUXNET sites use eddy covariance methods to measure the exchanges of carbon dioxide (CO₂), water vapor, and energy between terrestrial ecosystems and the atmosphere (Baldocchi 2003). Eddy covariance data at 30-minute frequency are typically maintained not by FLUXNET, but by individual towers. Contributing to FLUXNET enables standardized data processing, gap-filling, and formats (ORNL DACC 2015).

The FLUXNET database contains information about tower location and site characteristics as well as data availability.

The four variables from the flux towers used in this study include gross primary production (GPP), net ecosystem exchange (NEE) of CO₂, latent heat flux (LH) and sensible heat flux (SH). GPP is the total amount of carbon fixed during photosynthesis or the uptake of carbon. NEE is the GPP minus the RE. RE is the carbon losses due to respiration which includes both autotrophic and heterotrophic respiration. Autotrophic respiration is the loss of carbon from plants due to the costs of growth and maintenance. Heterotrophic respiration is the loss of carbon by soil organisms as they decompose organic matter. NEE values are negative when the plant is assimilating and taking up carbon, while positive NEE values mean that the ecosystem has more respiration than assimilation. LH and SH are turbulent energy fluxes that balance radiation gain by the land surface.

The 14-day rolling mean values of these four variables (NEE, GPP, LH and SH) were chosen to aid in the evaluation of the onset and duration of drought in the model compared to observations from 2010-2012. Based on the limited availability of flux tower data during this three-year timeframe, only two flux tower sites were used in this study. However, it is fortunate that these two sites represent the most extreme ends (New Mexico and Kansas) of the climate variability in this domain. The first flux tower site is the Sevilleta Desert Grassland in the Sevilleta National Wildlife Refuge in central New Mexico. Sevilleta is an arid-steppe, cold C4 grassland (ORNL DAAC 2015). The second flux tower site, Konza Prairie research site in eastern Kansas, is a mesic, tall-grass C4 grassland (ORNL DAAC 2015).

2.3 Seasonal Mean LAI and Water Deficit Calculations

This study focuses on precipitation and drought, which are key factors for grasslands. To investigate the relationship between precipitation and LAI, we have created plots of LAI versus precipitation. To do this, the growing-season mean LAI from every year over a 15-year time-period was used, in an effort to focus on the main seasonal features and interannual variability. The growing-season LAI was calculated by removing the lower 25% of the LAI values and then taking the annual mean from the remaining values. This was done for each grassland site from both SiB4 and MODIS.

Annual mean precipitation was used because it is well-known that there is relationship in region of this domain between the mean annual precipitation and the annual net primary productivity (ANPP) across sites from arid to mesic ecosystems (Sala et al., 1998; Knapp and Smith 2001; Huxman et al., 2004; Moran et al., 2014). ANPP is directly proportional to the maximum LAI. These seasonal mean LAI values were also used to create the anomaly plots of LAI versus the annual precipitation anomaly from SiB4 and MODIS at 9 grassland sites over 15 years, which is 135-site years of data. Finally, these anomaly values were broken down into the individual years of 2010, 2011 and 2012 to determine how well grasslands respond to drought.

Another drought indicator value, water deficit, was calculated at each site across the domain. Values of the water deficit were calculated by taking the rolling sum of the previous 100 days of the difference of precipitation and potential evapotranspiration (PET) over the 2010-2012 time period we are focusing on. From Blair et al. (2014), the ratio of the precipitation to the potential (PET) often is a better predictor of the ecological properties and process rates than just annual precipitation alone. Drier conditions occur when the PET is greater than the precipitation and those drier conditions can worsen over time. The PET was calculated using an

adapted Thornthwaite scheme for estimating the daily potential evapotranspiration from Pereira and Pruitt (2004). These calculations required temperature data and the daylength, also known as the photoperiod for each day. Other windows of the rolling sum were also tested, such as a 60-day versus the used 100-day window, but it was determined that these windows produced a similar trend of water deficit values just with different severities.

2.4 Simple Biosphere Model Version 4 (SiB4) Background

SiB4 is a comprehensive model of exchanges of heat developed for water, radiation, momentum and carbon used in global climate models. SiB4 predicts latent heat, sensible heat, net ecosystem exchange (NEE), gross primary productivity (GPP), leaf area index (LAI), litter and soil carbon from temperature, specific humidity, longwave radiation, shortwave radiation and wind speed. Conclusions from this study have been aiding the ongoing modifications and improvements of SiB4 (Haynes et al., 2016). SiB4 is modified from SiB3 (Baker et al. 2003; Denning et al. 1996, Sellers et al. 1996).

There were some key changes in SiB4 from SiB3 that are important to note including switching from biomes to plant functional types (PFTs), adding tiles for fractional coverage per grid cell (for example, one grid cell can have 20% C3 grass and 80% C4 grass), and introducing defined phenology stages (ex. leaf-out, senescence). SiB4 combines prognostic phenology, plant physiology, and ecosystem biogeochemistry. SiB4 is a land surface model that seeks to improve the estimates of carbon sources and carbon sinks (carbon cycle) as well as terrestrial fluxes of energy, moisture and momentum. The timing of carbon uptake and release is controlled by plant physiological processes such as temperature, moisture and light (Scheifinger et al., 2002; Larcher, 2003). Seasonal and inter-annual climatic variations influence the timing of plant

development, which in turn influences the temporal variability in ecosystem productivity (Baldocchi et al., 2001; Richardson et al., 2010).

Figure 16 illustrates how SiB4 works to supplement the text. SiB4 incorporated carbon pools by modifying the SiB-CASA scheme (Schaefer et al. 2008). There are five live carbon pools (leaf, fine root, coarse root, wood, product) and six dead carbon pools (coarse woody debris, metabolic litter, structural litter, soil litter, soil slow, soil armored). The live and dead carbon pools are illustrated in Figure 16 by the green and dark tan boxes, respectively. SiB4 predicts phenology to produce values of consistent carbon fluxes, pools and leaf area index (LAI) and calculates sub-hourly fluxes and updates phenology/pools daily. Prognostic phenology models can be used to investigate the relationship between climate variables, plant development and carbon fluxes, in addition to providing continuous estimates of the biophysical state (Stockli et al., 2008, 2011; Jolly et al., 2005).

SiB4 calculates fluxes of photosynthesis and respiration every time-step. Photosynthesis is predicted from enzyme kinetics coupled to stomatal physiology following Farquhar et al. (1980) and Collatz et al. (1991, 1992). SiB4 utilizes dynamic prognostic phenology and five phenology stages (phenostages) after the dormancy period (Stage 0). The five phenostages in order, include leaf-out (Stage 1), growth, maturity, stress and senescence (Stage 5). The three primary determinants for the start of the growing season (shown in Figure 16 referred to as Leaf-Out Initiation) include temperature, soil moisture, and light (day-length). Once in a growing season, the phenostage is determined by a leaf cost-to-benefit factor and an assimilation factor. The leaf cost-to-benefit factor combines the relationship between LAI and the fraction of photosynthetically active radiation (FPAR) with climatological and real-time stresses to determine the phenology stage when the plant is growing (leaf-out, growth and maturity phases).

The assimilation factor is used to determine the phenology stage when the rate of assimilation is decreasing (stress, senescence). These values, combined with further adjustments for temperature and moisture, are used to allocate the assimilated carbon to the live pools.

Autotrophic respiration from the live pools includes growth respiration and maintenance respiration, which is calculated every time-step. The transfer of carbon from the live to dead carbon pools is based on phenology stage, temperature and moisture. In regards to the six dead carbon pools, the heterotrophic respiration and transfer from these pools depends on PFT-dependent turnover times that are modified for each site based on temperature and soil moisture factors, as well as carbon pool size. The gains and losses for each carbon pool are summed daily, and the carbon pools are updated at midnight (local time). The vertical distribution of all carbon pools located in the soil is based on the rooting profile of the PFT. For grasslands, the live above ground biomass is used to calculate the LAI, which is used to calculate the carbon assimilation, completing the carbon cycle.

There are three stress parameters in SiB4 that hinder stomatal conductance (such as during drought or at end of the growing season) including temperatures stress, humidity stress and root zone water stress. The soil moisture within SiB4 does respond to change in precipitation but it also depends on soil characteristics. Once the soil moisture is calculated, then the root zone water stress parameter can be calculated from the root-density-weighted excess of soil moisture above the wilting point in each layer of soil. Finally, then the running mean of this soil moisture stress is calculated and it has to surpass a PFT-specific value in order to start growing. For example, if the start of the growing season is delayed in SiB4, that could result in a shift of timing in the magnitude of carbon assimilation (change timing of phenostages).

SiB4 is a self-consistent global land surface model that requires minimal input data as shown in Figure 17 such as weather, soil properties and PFT. The input data of soil properties/characteristics comes from the 0.5° Global Gridded Surfaces of Selected Soil Characteristics (IGBP-DIS) dataset which include the percent fraction of percentages of silt, clay and sand as well as the soil reflectance (Global Soil Data Task Group 2000). From these values, the Clapp and Hornberger (1978) power curve equations were used to obtain more soil parameters such as porosity, conductance, field capacity and wilting point. Finally, the input weather data is from NASA's Modern Era Retrospective-Analysis for Research and Applications (MERRA - Reinecker et. al 2011). MERRA is a retrospective-analysis that integrates a variety of observing systems with numerical models to produce a temporal and spatially consistent synthesis of observations and analysis of variables not easily observed, which is ideal for investigating climate variability globally.

In the SiB4 model, the MERRA variables used include hourly temperature, wind speed, shortwave radiation, longwave radiation, precipitation and specific humidity with a grid cell of 0.5° by 0.67° over the whole globe. MERRA precipitation is then rescaled by the monthly values from the Global Precipitation Climatology Project (GPCP) version 1.2 product (Huffman et al., 2001). That product has monthly precipitation from an average of rain gauges in 1° by 1° grid cells. For every MERRA gridcell, monthly total precipitation is scaled to the nearest GPCP monthly estimate. Finally the meteorological input data is re-scaled to 0.5° by 0.5°. For this study, we have used the data from the gridcell containing each tower.

It is well-known that re-analysis precipitation products such as MERRA have a tendency to smear out the precipitation. For example, there are many small precipitation events in MERRA as opposed to large, isolated precipitation events (Ashouri et al. 2015). Given this, it is expected

that there will be discrepancies in the timing of the rainfall within each month between MERRA and local observations. Since in this study we are focusing the seasonality and the interannual variability, the MERRA monthly-scaled by GPCP is sufficient because both the rain gauge data and MERRA are equal on the monthly timescale.

The plant functional type (PFT) used at each tower is the associated PFT representing the vegetation coverage at that tower. We have selected sites that are dominated by C3 grass and C4 grass. In the model, like the real world, C4 and C3 have different photosynthetic pathways and different responses to heat stress: C4 has a higher tolerance to warmer temperatures than C3. One key difference is that unlike the real world, SiB4 does not use different root structure/depths between C3 and C4, which could alter the root stress in periods of drought (Blair et al. 2013). Terrestrial biosphere models (TMBs) like SiB4, do have limitations because the models can only resolve PFTs but not the different species of the PFTs, which could have a significant impact on simulated variables such as soil moisture, root zone stress, etc. In addition to input data, as with all land surface models, SiB4 requires a variety of parameters. The parameters and their associated values are provided in Haynes et al. (2016). It should be noted that since SiB4 is a global model, it is not calibrated for specific sites.

Grazing has been introduced into this newest version of SiB4. To calculate the impact of grazing, first spin-up runs of 18 years were used to determine the net primary production. Second, we calculated a daily grazing amount that was equal to 40% of the 18-year NPP divided by the total number of grazing days, where a day was considered to be grazed if the LAI was above 0.7. This calculated daily grazing rate was then used in the simulations, and on the appropriate days carbon was transferred from the above-ground pools (leaf, stem, product) to respiration and other carbon pools.

CHAPTER 3: RESULTS AND DISCUSSION

3.1 Climatological Wet-Dry Gradient

The U.S. Great Plains has a large west-east climatological gradient from the dry climate in the west at Sevilleta, New Mexico to the wet climate in the eastern side of the domain (Konza Prairie, Kansas) as shown in Figure 5. Some of the chosen grassland sites including Sevilleta and Konza are also instrumented with phenocameras. According to White et al. (2009), the current methods used to analyze phenology include ground-truth direct observations of plants (National Phenology Network), eddy flux towers, digital cameras/remotely sensed data such as phenocameras and MODIS and terrestrial biosphere models such as SiB4. In an attempt to improve the timing of phenology in terrestrial biosphere models and remote sensing platforms, phenocameras from the PhenoCam network can be utilized. Phenocameras are high-resolution digital cameras placed on towers that provide images every half an hour (Richardson et al., 2009).

Figures 18 and 19 are phenocameras images from Konza Prairie, Kansas site on August 11th 2012 (first year data was available) which was a drought year and August 11th 2015, a non-drought year. Figure 20 is the image from Sevilleta, New Mexico on August 11th 2015 during a non-drought year (first year data was available). The difference in vegetation is apparent between the two extreme sites with the drought in 2012 the vegetation appearing browner and more sparsely vegetated (Figure 18). This corresponds well with the calculated LAI and flux values that will be explained later on.

Now, let's focus on how these grassland sites respond to the 15-year mean precipitation over this large precipitation gradient. The first question posed in this study was as follows: ***Over the 15-year MODIS record at the nine sites across the dry-to-wet gradient, is the seasonal mean***

LAI linear with respect to annual mean precipitation? Figure 21 shows the 2000-2014 seasonal mean LAI versus the annual mean precipitation for both SiB4 and MODIS. Comparing mean precipitation against seasonal mean LAI reveals a strikingly linear relationship between seasonal mean LAI and precipitation across the precipitation gradient in the U.S. Although there is some site variability, the desert grassland (US-Seg), has minimal precipitation and minimal LAI as shown in the phenocameras image. As the precipitation increases moving eastward, the LAI also increases nearly linearly.

In the mid-region of this study, an annual precipitation of ~600 mm corresponds with an LAI of ~1.0 in SiB4. Shifting east again towards the productive sites, both precipitation and LAI increase together so that at sites with ~1000 mm of precipitation (4x the desert sites) the LAI is ~2.0 for SiB4. The slope in SiB4 was $0.001825 \text{ m}^2\text{m}^{-2}$ per millimeter or $1.825 \text{ m}^2\text{m}^{-2}$ per meter meaning that for every 1 meter of precipitation, there is a gain of 1.825 units of LAI. The slope of MODIS was $0.00179 \text{ m}^2\text{m}^{-2}$ per mm or $1.79 \text{ m}^2\text{m}^{-2}$ per meter meaning that for every 1 meter of precipitation, there is a gain of 1.79 units of LAI. In SiB4, the R^2 equals 0.800 and for MODIS, the R^2 equals 0.700.

These R^2 values explain 70-80% of the variance which proves that the strength of this relationship of LAI versus precipitation is significant in both MODIS and SiB4. This may indicate that while temperature and evaporation are important variables in the growing season, these plots show that precipitation is the dominant factor, and that there is a linear relationship between annual precipitation and seasonal mean LAI

SiB4 produces the same linear response of LAI to precipitation as the observations (MODIS) with a difference in slope of <0.00003 . This could indicate that the model has skill in predicting grasslands, the LAI and the grassland response to precipitation. Even though the slopes are

almost identical, SiB4 does overestimate the magnitude of the LAI, as seen by the offset from the MODIS data. However, this offset is consistent across all sites, meaning that SiB4 has a bias in LAI. This bias is particularly noticeable in the C3 grass parameters given that the two extreme (C4) grass sites seem to be in the most agreement compared to the mixed grassland and the lone C3 grassland site, US-Ctn (K. Haynes, personal communication).

3.2 Seasonality

3.2.1 Leaf Area Index (LAI)

From 2010 to 2012, SiB4 simulated the known west-to-east gradients in grassland productivity as shown in the LAI (Figures 22-30) values from the dry climate in the west (Sevilleta – Fig. 22) to the wet climate in the eastern side of the domain (Konza – Figure 30). Overall, SiB4 does fairly well in calculating values of the leaf area index (LAI) compared to observations from MODIS. SiB4 generally overestimated the value of LAI compared to the observations in the majority of the grassland sites similar to the pattern seen in the 15-year mean results shown in Figure 21. The maximum of the LAI (peak of season) is also generally too high in SiB4. SiB4 did fairly well capturing the interannual variability in addition to the seasonal cycle (timing of onset and senescence). However, the C4 grassland sites (Sevilleta and Konza) at the extremes of the climatological gradient in this domain seem to perform better in the model than the mixed grassland sites and the one C3 grassland site in South Dakota (Fig. 25) in the middle of this domain.

The accumulative water deficit was chosen as another drought indicator because a large amount of water deficit means that there is a higher amount of potential evapotranspiration compared to precipitation that over time could lead to drought conditions. As expected, when

sites experienced drought conditions, there were large decreases in LAI with large negative values of water deficit (more potential evapotranspiration than precipitation). The WD values do not work quite as well at US-Seg given that the growing season and precipitation are based on individual events, not seasonality.

Now to take a look at all nine sites in detail in regards to the LAI and water deficit (WD) values, starting with the driest, western site of Sevilleta (US-Seg). US-Seg has low values of LAI as expected in both MODIS and the model; see indications that it is water stressed every year. 2011 was the least productive year with almost no growing season compared to 2010 and 2012. There was a drought in 2011 according to the National Drought Mitigation Center (NDMC) as shown in Figures 7-10. The northern mixed grassland sites (Figures 23–26) include the Shortgrass Steppe in northeast Colorado (US-SGS), Sandhills in Nebraska (US-SdH), Cottonwood in central South Dakota (US-Ctn) and Brookings in eastern South Dakota (US-Bkg). US-SGS is the second least productive site within this domain. Both MODIS and SiB4 indicate that the maximum LAI values dropped by more than half in 2012 compared to 2010 and 2011 while the accumulative water deficit decreased from around a 20-30mm in 2010 to about -550mm in 2011 at US-SGS, US-SdH and US-Ctn. This agrees with the drought maps from the NDMC shown in Figures 12-14 that show that a drought occurred at these sites in 2012. US-Bkg (Fig. 26) also shows a drop in 2012 in the LAI and WD compared to 2010 and 2011 but not as severe as the other three northern mixed grassland sites.

SiB4 does seem to get the timing of the seasonality correct at these northern mixed grassland sites. However, the model does end the growing season in 2012 at US-Bkg a bit earlier than MODIS though. In addition, the model does overestimate the LAI values at the peak of the growing season. The values of LAI in both the model and MODIS in these four northern

mixed grassland sites go to zero in the winter when there are cold enough temperatures that grasses do not grow.

This is in contrast with the southern mixed grasses including the ARM site in Oklahoma (US-Arc) and at Freeman, Texas (US-Fr1) shown in Figures 27-28. While SiB4 does go to zero at these two sites, MODIS does not. This indicates that the model at the warmer sites is underestimating the LAI because the model is not realizing that in the winter in this area, there can still be some grass growing due to warm enough temperatures. In addition, MODIS LAI values include other PFTs than just grasslands so that could explain some of the discrepancies between model and observations.

In US-Arc, the maximum LAI in SiB4 dropped from 2.5 in 2010 to 1.3 in 2011. US-Fr1 also shows a decrease of maximum LAI from about 3.5 in 2010 and 2012 to only .75 in 2011. The MODIS at both sites indicated a dip in the LAI in 2011 as well but the decrease was not as dramatic, again probably due to the fact that MODIS is seeing vegetation types other than just grassland PFTs. The WD values dropped significantly in 2011 at US-Arc from about a zero WD in 2010 to -550mm in 2011 and had a similar water deficit in 2012. The WD values at US-Fr1 also dropped in 2011 to about -500mm but there is some recovery of water deficit in 2012.

Compared to 2010, there is a shortened growing season in 2011 in US-Arc and US-Fr1 in conjunction with the drought (Figures 7-10). In 2012 at US-Fr1, the model ended the season too abruptly compared to MODIS and WD which could be due to end of season stresses in the model such as temperature and moisture stress. Even though it appears that from the WD values that there is potentially enough water to sustain growth, SiB4 is unable to start growing again, so this indicates that there is an issue with the temperature stress in the model. Compared to the other sites, SiB4 has the most difficulty with the seasonality in US-Arc and US-Fr1. This could be due

to the model being too sensitive to temperatures; it doesn't get nearly as cold at these two sites compared to the others. Another issue could be that the MODIS covers a 7km by 7km swath and from further investigation, these two sites have another vegetation types that are altering the values of LAI in the MODIS while SiB4 only uses the two grassland PFTs. For example, at Freeman Ranch in Texas, this site is next to woodland and juniper sites.

The final two sites are the tallgrass prairies sites in eastern Kansas: Walnut Creek (US-Wlr) and Konza Prairie (US-Kon) shown in Figures 29-30. These two sites are the most productive in this domain with maximum LAIs at about 3 within this timeframe compared to the maximum LAI value of 0.25 at the desert site (US-Seg). US-Wlr shows a dip in production in 2011 and 2012 compared to 2010 with a decrease of about 0.5 units of LAI in the model. The WD values drop to about -400mm in 2011 and 2012. US-Kon shows a decrease of the maximum LAI in 2012 compared to 2010 and 2011. There is also a shortened growing season in conjunction with a significant water deficit that corresponds with the known drought conditions (Figures 13-14). Although, it is important to note that MODIS cuts the growing season short in 2011 unlike SiB4. While the pattern in general agrees between MODIS and SiB4 at these two sites, there is an issue in 2012 in regards to the shoulder season (the end of the season).

Overall for all sites, there are some WD dips during summer due to the seasonality which is when it would be normal to see some water deficit. However, periods of large WD severity in combination with low LAI values were of the most interest because it indicated drought. In some cases, SiB4 seems to have issues with the shoulder seasons, the time periods at the beginning and end of the main growing season. Cases of early and delayed start of the growing season in SiB4 could be due to the three triggers that start the growth: temperature, soil moisture and daylength.

In some cases, SiB4 also ramps down the growing season too quickly towards the end of the season (eg. US-Arc in 2012 and US-Kon in 2012). There are two combined ideas that explain this. The first part is that the model is calculating low enough amounts of carbon assimilation towards the end of the growing season that it cannot continue to grow. Once the values of respiration dominate over assimilation, the plant goes into the senescence phase and it doesn't recover due to the three stress factors (humidity, temperature and root zone moisture). The second part of the explanation is that there are differences from SiB4 versus observations on the timing and magnitude of the transfer of live carbon pools to dead carbon pools.

3.2.2. Energy and Carbon Fluxes

The two extreme sites of US-Seg and US-Kon were further explored to analyze and discuss some additional differences between SiB4, MODIS and the flux towers. The precipitation from both MERRA and the U.S. Climate Reference Network (USCRN - Diamond et. al. 2013) at these two sites (US-Seg and US-Kon) is illustrated in Figures 31-32. Konza receives more precipitation than Sevilleta, which is what was expected given the phenocameras images (Figures 18-20). Note that the y-axes have different scales in order to see the individual precipitation events at Sevilleta.

From these precipitation data, precipitation at Konza is strongly seasonal, with a summer maximum and winter minimum; this seasonal cycle is less obvious in Sevilleta. At Sevilleta, there is a large growth response to individual precipitation events which one may not know until further looking at these rain events and also in the LAI values. The timing of the climate variability (in this case, the timing of the precipitation event) is just as important, if not more

important, than its magnitude (Craine et al., 2012). For example, if the precipitation event occurs during the shoulder seasons, SiB4 may not have a growth response.

While most temperate grassland sites have a strong seasonal cycle, US-Seg (desert grassland) is driven by individual precipitation events. Using precipitation data (Fig. 31), these significant events that occurred in the growing season have been numbered on all of the US-Seg plots to aid in the understanding. Two significant precipitation events (1 and 2) occurred in the mid-part of the growing season in 2010 and 2012 while medium-sized events (3 and 4) occurred during the shoulder seasons of 2010. US-Seg had the most production in 2010, a year with no indication of drought conditions. 2011 had very little growth, which was a combination of a severe drought in the overall southern region of this domain as well as an extreme freezing event in February 2011 (personal communication, Dr. Marcy Litvak, PI of Sevilleta LTER).

Overall, the carbon and energy flux values between the model and the flux tower do match up fairly well (Figures 33–36). The NEE values (Fig. 33) are low but do have the same pattern as the individual rain events. However, there are some differences in the timing of the main growing season in 2012 and the shoulder seasons in 2010. The GPP (Fig. 34) values are also quite low in both with a maximum less than $2.0 \text{ micromoles of C m}^{-2} \text{ s}^{-2}$; these small maximums matched well with the precipitation events. The latent heat values look remarkably good and again, LH follows the pattern of the main rain events (Fig. 35). As expected in a desert site, the sensible heat dominates over the latent heat, again can even see where the main two precipitation events (1 and 2) occur where the SH drops suddenly in 2010 and 2012 (Fig. 36). The daily Bowen ratio used in many drought studies (the ratio of sensible to latent heat) is at times greater than 10 which is expected in desert/semi-arid locations. 2012 showed indications of production

but also experienced some drought conditions that will be explained later on using the anomaly plots.

Figures 37- 40 illustrate the linearity between the model and flux tower for the four flux variables at US-Seg over the same three-year time period. While the model shows some skill, there is still need for improvement. Figure 37, the NEE, has an R^2 value of 0.3273. This low value reflects the discrepancy in 2011 between the model and the observations due to the almost complete lack of growth during the extreme drought that year. However, the other three variables have higher correlation values with GPP having an R^2 value of 0.6975, LH having an R^2 value of 0.6349 and SH an R^2 value of 0.8346.

In contrast to US-Seg, US-Kon is a productive grassland with a clear seasonal cycle which is shown not only in the LAI and the precipitation plot, but also in the carbon and energy fluxes (Figures 41–44). The GPP is much higher in Konza (Fig. 42) compared to US-Seg (Fig. 34). Overall, SiB4 generally agrees with the flux tower data. In both the model and observations, the GPP has a strong seasonal cycle, the NEE is less than zero at midseason and the NEE is greater than zero in shoulder seasons (Fig. 41) when the respiration (RE) is greater than GPP ($NEE=GPP-RE$). The seasonal pattern of LH (Fig. 43) is similar to GPP while SH has its maximum in the shoulder seasons (Fig. 44). It is important note that the values of GPP could be a little low in model because the flux tower is in the productive annual burn site which this model does not include (no fire in model).

For the interannual variability, 2011 has a drop off in the observations of GPP and NEE with a larger drop in LH but not in the model. In 2012, both SiB4 and observations show reductions of GPP, NEE, LH and an increase in SH due to the significant drought that occurred (Figures 12-15). In the NEE plot of US-Kon (Fig. 41), the model is able to get the shape correct and even

capture the pulses of respiration before and after the growing season with the correct magnitude. The latent heat is remarkably good, can even see the significant precipitation events. There is a drop during 2012 that corresponds to the known drought (Fig. 43).

The sensible heat at US-Kon is lower than US-Seg which is expected. The sensible heat values in the model do simulate the general pattern of having a double peak during the shoulder seasons but does consistently underestimate the SH (Fig. 44). SH is greatest during the shoulder seasons (around March/April and October) when there is a significant amount of net radiation due to sparse vegetation cover on the surface. It is difficult for the model to remove water from soil in spring and fall when the surface of the ground is brown as opposed to green during the growing season. The underestimation of SH in the model suggests an underestimate of net radiation which is likely due to the overestimation of albedo at this particular site.

MODIS as well as the flux values indicate a shorter and less productive growing season compared to SiB4 in 2011 (Figure 30, 41–44). This is indicated by less uptake of CO₂ in the NEE values, lower LH values and lower GPP values. This difference of the length of growing season was further explored to see if it could be explained by the annual burning of Konza. The annual burn happened earlier on in the season (around March/April) so this hypothesis turned out to be false. As explained previously, this inhibition of plant growth in 2012 shown in the GPP plot is the result of low carbon assimilation values and the timing and magnitude transfer from live to dead carbon pool.

Figures 45- 48 illustrate the linearity between the model and flux tower for the four flux variables at US-Kon over the same three-year time period. While the model shows some skill, there is still need for improvement. In Figure 45, the NEE, has an R² value of 0.6445. The R² value for GPP is 0.8140, LH is 0.718 and SH is 0.4166. This low R² value in

sensible heat plot makes sense given the difference of values also shown in Figure 44.

Underestimation of SH in the model suggests an underestimate of net radiation which is likely due to the overestimation of albedo in the model at this particular site, probably due to insufficient retention of senescent grass.

3.3 Interannual Variability

To further explore the relationship between grassland and drought, the standardized anomalies of the seasonal mean LAI in both MODIS/Obs and SiB4 using the 15-year means were calculated and plotted against the standardized anomalies of the annual mean precipitation (Figures 49-50). The standardized seasonal LAI anomaly equals the seasonal mean LAI of a specific year minus the average seasonal mean LAI over the 15 years divided by the standard deviation of the average seasonal mean LAI over the 15 years. The standardized precipitation anomaly equals the mean precipitation of a specific year minus the average precipitation over the 15 years divided by the standard deviation of the mean precipitation over the 15 years. The standardized anomaly for each year for each site (or 135 site-years) was plotted for both Obs and SiB4.

Interestingly, there is also a linear relationship between the annual mean precipitation anomaly and the seasonal mean LAI anomaly. Again, MODIS and SiB4 have similar slopes. However, there is more scatter in the Obs compared to SiB4 which indicates that there are other controls of LAI. The R^2 values also indicate that about half of the anomaly can be explained by precipitation but this is still significant considering all the factors that go into growth such as different species, temperature, evapotranspiration, grazing, fire, other disturbances, etc. Overall,

this indicates that there is a linear response of grassland LAI anomalies to precipitation anomalies.

To match the timeframe of the LAI plots, the anomalies for the individual years of 2010, 2011 and 2012 were analyzed (Figure 51-53). As indicated in the LAI plots, most sites were drought-free in 2010. Although, we could be seeing signs of the drought that started to develop in the southern part of the domain towards the end of the year that led into 2011 (ex. Freeman, Texas – US-Fr1 site). In 2011, the southern sites experience drought while the northern and eastern sites did not indicate drought conditions. Given that Texas and Oklahoma had record dry conditions and record high temperatures in 2011 (NCDC 2012), it is known that temperature in addition to precipitation is an important factor when it comes to drought.

Then in 2012, all nine sites experienced drought with Texas slowly coming out of the drought. It is important to remember that while the late-season 2010 drought continued into 2011 in the southern sites, the 2012 drought was a flash drought that was not a continuation from the previous year. These plots prove further that SiB4 did well in capturing the interannual variability. It simulated drought at the appropriate sites on the correct year.

Given the severity of drought in 2012, the second question posed in this study was as follows: ***During the 2012 drought, do reductions in the seasonal mean LAI in response to large decrease in precipitation fall on the same line as the average response of LAI to climatological precipitation?*** Figure 54 illustrates the 15-year mean values for the seasonal mean LAI vs. annual mean precipitation values (same as Figure 21) displayed as closed square and circles. In addition, the LAI vs precipitation values for 2012 for each site are displayed as the OPEN squares (model) and circles (observations). This figure allows the user to easily see the difference of 2012 compared to the 15-year average. In response to the 2012 drought, all

nine sites maintained this same linear relationship even with a significant decrease in LAI and precipitation. For example, Konza in the gold color, decreased from ~ 1.75 LAI in both SiB4 and Obs from the 15-year mean to ~ 1.0 LAI in SiB4 and ~ 0.6 LAI in the observations, with a decrease of about 300 millimeters in precipitation in 2012. The linear relationship between LAI and precipitation did not break during periods of extreme drought.

The third question was as follows: *Does the model match the observations as shown in the first two questions?* Despite the consistent overestimation in LAI magnitude in the model compared to observations, the model was able to capture the same linear relationships as the observations in regards to the climatological gradient and the drought response as shown in Figures 21 and 54, respectively.

CHAPTER 4: CONCLUSIONS

Using grasslands across the U.S. Great Plains, we were able to investigate how grassland behavior changed across this region, which experiences a significant precipitation gradient.

There were three main questions that were addressed in this study:

- 1. Over the 15-year MODIS record at the nine sites across the dry-to-wet gradient, is the seasonal mean LAI linear with respect to annual mean precipitation?*
- 2. During the 2012 drought, do reductions in the seasonal mean LAI in response to large decrease in precipitation fall on the same line as the average response of LAI to climatological precipitation addressed in the first question?*
- 3. Does the model capture these relationships as in the observations addressed in the first two questions?*

There was an increase in LAI with increasing precipitation, which has a linear relationship in both the observations and the model using 15-years of data which answers the first main question. SiB4 generally overestimates the LAI compared to observations in the majority of the 9 chosen grassland sites. However, SiB4 did fairly well in capturing the interannual variability in addition to the seasonal cycle in most sites. In Sevilleta the desert site, there was low precipitation, low LAI, low fluxes and a daily Bowen ratio at times above 10. The growth was based on individual precipitation events, not the seasonal cycle.

As the precipitation increases moving eastward in this domain, the LAI also increases nearly linearly. The LAI values from 2010-2012 from model and observations as well as the accumulative water deficit were analyzed at four northern mixed grasses, two southern mixed grasses and two tall-grass sites in eastern Kansas. At the four northern mixed grassland sites located in Colorado, Nebraska, and South Dakota, the model does seem to get the timing of the

seasonality correct. The model also accurately indicated that there were drought conditions in 2012 in all 4 of these sites.

The two southern mixed grass sites are located in Oklahoma and Texas. SiB4 does not capture the seasonality as well as these two sites compared to the four northern mixed grassland site but it accurately indicated drought conditions in 2011. The last two sites of interest called tall-grass prairies (the most productive sites) are located in eastern Kansas. There was a strong seasonal cycle, large amounts of precipitation, large LAI, and large flux values. There was more latent heat than sensible heat due to evapotranspiration at mid-summer, so the daily Bowen ratio was less than 1. Again, the model generally captures the seasonality and the drought in 2012. However, there are some differences in the timing of the end of the growing season in 2011 and with the shoulder season in 2012.

In addition to studying the general response of grassland productivity to precipitation, this study investigates the response of grasslands to drought. This region experienced significant drought at particular sites in 2011 and 2012, which is recent enough to allow us to look at those events more in depth. To answer the question if the linear relationship between LAI and precipitation breaks during periods of extreme drought, it does not appear to break linearity in this study by comparing the response of the sites in the 2012 drought compared to the 15-year mean which answers the second main question of this study. Again, there was the same linear response in the anomaly plots and that relationship is the same in the model and the observations. For both the model and observations, one-half of the anomaly can be explained by precipitation but this is still significant considering all the factors that go into growth such as different species, temperature, evapotranspiration, grazing, fire, other disturbances, etc

Overall, this study indicates that there is a linear response to grassland LAI to precipitation in both the model and the observations which answers the third main question of this study. SiB4 has a bias in the magnitude of seasonal-mean LAI, but it has the same response to precipitation, and shows the ability to capture the behavior of grasslands both across a dry-wet gradient and for a specific drought event. Finally, SiB4 shows improvement in capturing the seasonality and especially the interannual variability compared to earlier terrestrial biosphere models (Schwalm et al., 2010; Schaefer et al., 2012; Razcka et al., 2013).

CHAPTER 5: FUTURE WORK

The U.S. Great Plains region was chosen for the large precipitation gradient from west-east and the time frame of 2010-2012 was chosen due to the significant drought conditions. However, this study was limited to only two flux tower C4 grassland sites, Konza and Sevilleta, due to data availability. It would be beneficial to include additional flux tower sites in further studies. There is also a need to evaluate other regions around the globe with significant precipitation gradient to see if they have the same linear relationship between LAI and precipitation values in grasslands as found in this study. Are they dominated by this same linear response? We know from this study that we are capturing the overall behavior of annual net primary productivity (ANPP) values (capturing the extreme ends, low ANPP/low LAI at US-Seg and high ANPP/LAI at US-Kon). Values of the ANPP are available at certain Long-Term Ecological Research (LTER) sites in this domain.

While this study focuses on the ANPP (directly related to the maximum LAI) of individual years, it could also be beneficial to plot the average of two years of ANPP to improve the relationship of ANPP versus precipitation in the short-term according to Moran et al. (2014). Moran et al. (2014) found that the ANPP responded primarily to the current-year precipitation in the extreme sites while the mesic sites responded mainly to the previous-year ANPP.

It would also be a good idea to find data for belowground net primary production (BNPP) in addition to ANPP. The carbon cycle also depends on the belowground carbon pools which include three dead carbon pools (soil carbon being the largest) and one live carbon pool (live roots). If have measurements of all the four below ground carbon pools, then one can determine the root turnover time which would help the allocation of carbon in the model (how much and when). In addition, another area of exploration could be how much drought years alter the

ANPP/BNPP. Another idea is that these relationships could be explored beyond the grassland sites into other PFTs. Given that grasslands are highly sensitive to disturbances such as grazing and fire, grazing amounts could be varied in the model and fire could be introduced into model for sites that have prescribed burns (ex. Konza Prairie has annual burn in April).

In addition, in multiple sites/years, there is still room for improvement on the shoulder season in SiB4 compared to MODIS and the flux tower data. To improve this, modifications could be made in SiB4 in regards to how it calculates respiration and the transfer of live and dead carbon pools towards the end of the season. Lastly, the next thing to investigate is the root zone water stress parameter because it directly relates to soil moisture and, therefore, drought. Improving this parameter could also improve the issues that are prevalent in the shoulder seasons. It is quite possible that the soil in the model is drying out too quickly, leading to more water stress, which could be an artifact of the wrong soil moisture and root zone water stress.

TABLES AND FIGURES

Table 1. Details of the Grassland Sites and Plant Functional Type (PFT).

| Tower | Site Name | Site Location | Lat | Lon | Description |
|--------------|-------------------------------|----------------------|------------|------------|---|
| US-Arc | ARM SGP Control Site | Oklahoma | 35.55 | -98.04 | Mixed Grass Prairie with Grazing (40% C3, 60% C4) |
| US-Bkg | Brookings | South Dakota | 44.34 | -96.84 | Mixed Grass Prairie with Grazing (40% C3, 60% C4) |
| US-Ctn | Cottonwood | South Dakota | 43.95 | -101.85 | Arid Steppe Cold Grassland with Grazing (100% C3) |
| US-FR1 | Freeman Ranch | Texas | 29.93 | -98.01 | Mixed Grass Prairie with Grazing (30% C3, 70% C4) |
| US-Kon | Konza Prairie | Kansas | 39.08 | -96.56 | Tall Grass Prairie with Grazing Burned Annually (100% C4) |
| US-SdH | Nebraska SandHills Dry Valley | Nebraska | 42.07 | -101.41 | Mixed Grass Prairie with Grazing (40% C3, 60% C4) |
| US-Seg | Sevilleta Desert Grassland | New Mexico | 34.36 | -106.7 | Arid Steppe Cold Grassland (100% C4) |
| US-SGS | Shortgrass Steppe LTER | Colorado | 40.81 | -104.19 | Arid Steppe Cold Grassland with Grazing (15% C3, 85% C4) |
| US-Wlr | Walnut River Watershed | Kansas | 37.52 | -96.86 | Mixed Grass Prairie with Grazing (35% C3, 65% C4) |

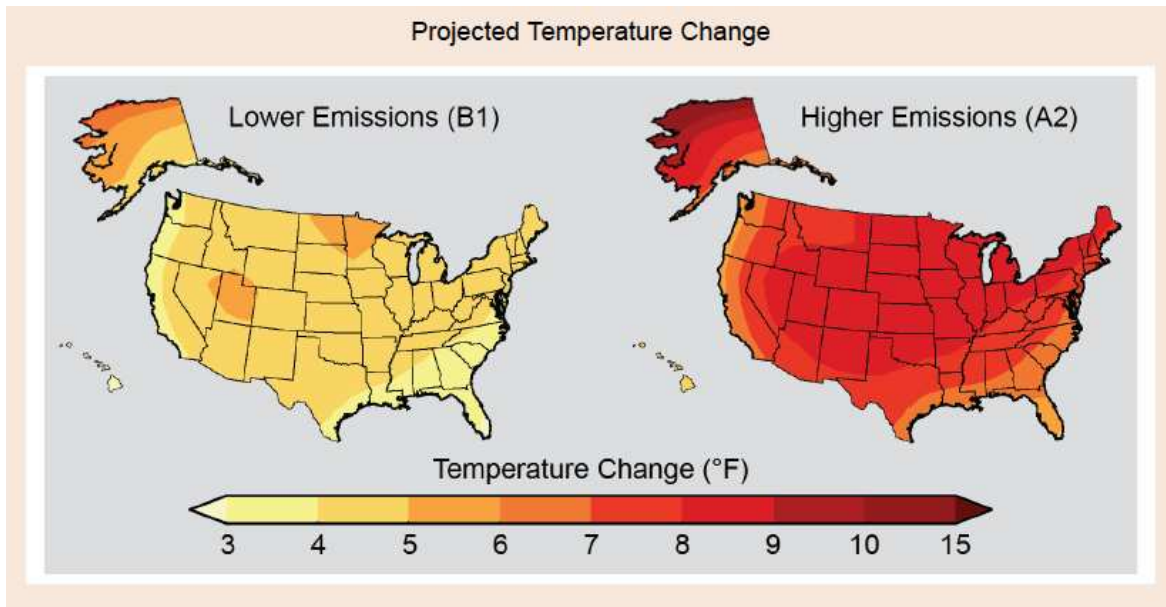


Figure 1. Projected change in average surface air temperature in the later part of this century (2071-2099) relative to the later part of the last century (1970-1999) under a scenario that assumes low emission scenario (B1, left) and a higher emissions scenario that assumes continued increases in global emissions (A2, right). Walsh et al., 2014.

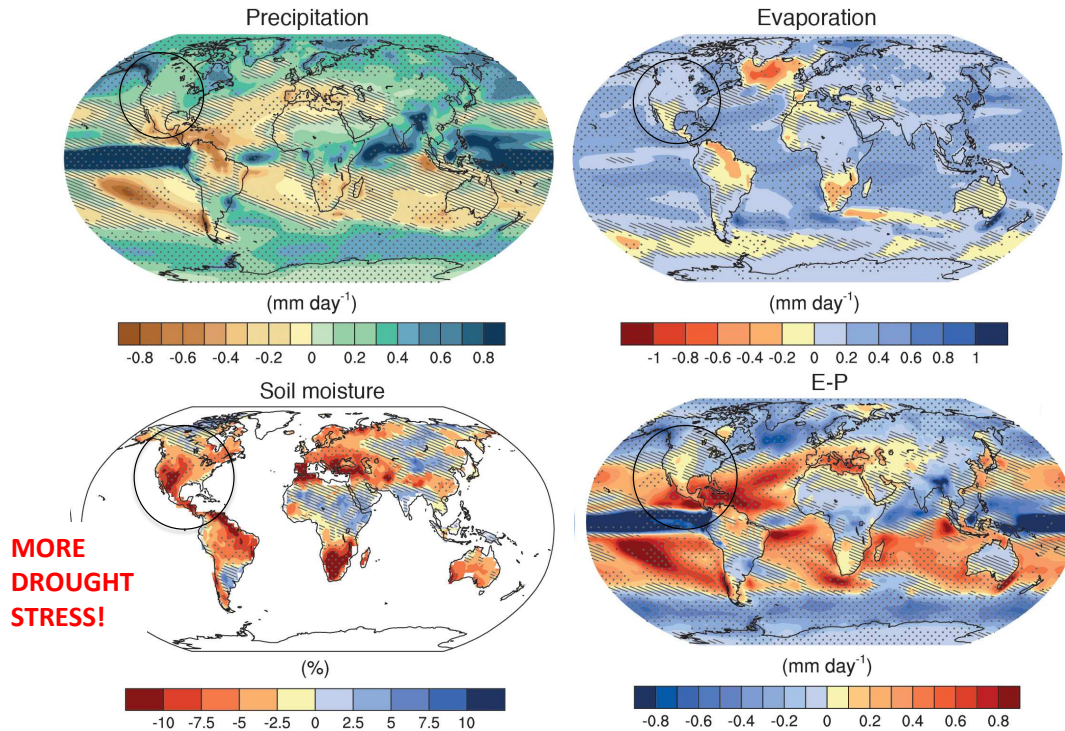


Figure 2. IPCC AR5 Change in Water Cycle using the High Emission Scenario (RCP 8.5). Annual mean changes in precipitation (P), evaporation (E), E – P, and soil moisture for 2081–2100 relative to 1986–2005. Hatching indicates regions where the multi-model mean change is less than one standard deviation of internal variability. Stippling indicates regions where the multi-model mean change is greater than two standard deviations of internal variability and where 90% of models agree on the sign of change. Stocker et al., 2013.

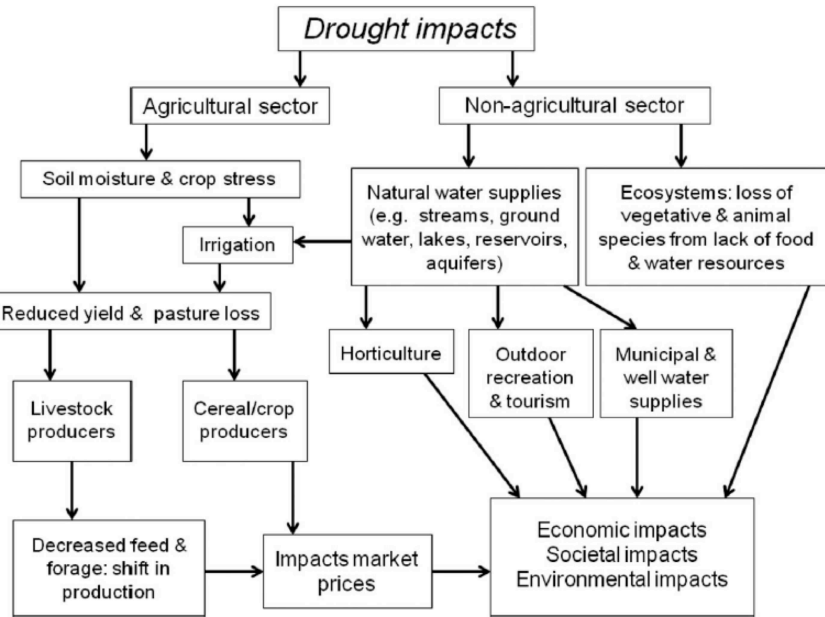


Figure 3. Drought impacts on the economy, societies and the environment moving through time from the top to the bottom of the chart. Kellner and Niyogi 2014.

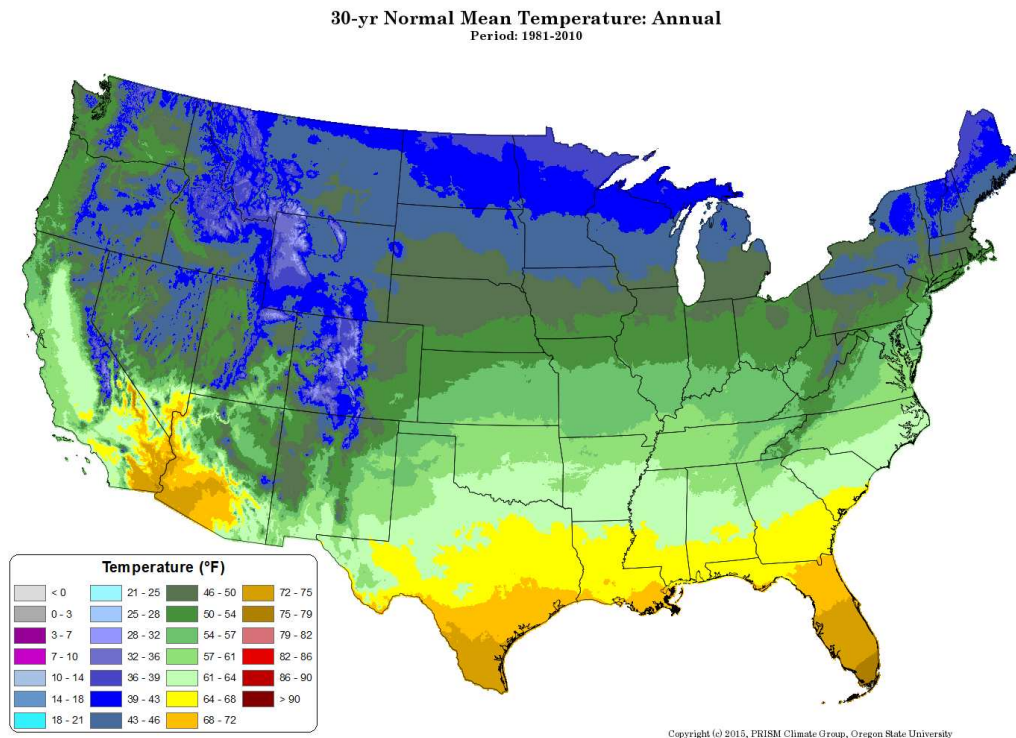


Figure 4. Parameter-elevation Relationships on Independent Slopes Model (PRISM) 30-year (1981-2010) Average Annual Temperature in Farenheit. From (<http://www.prism.oregonstate.edu/normals>). PRISM.

30-yr Normal Precipitation: Annual
 Period: 1981-2010

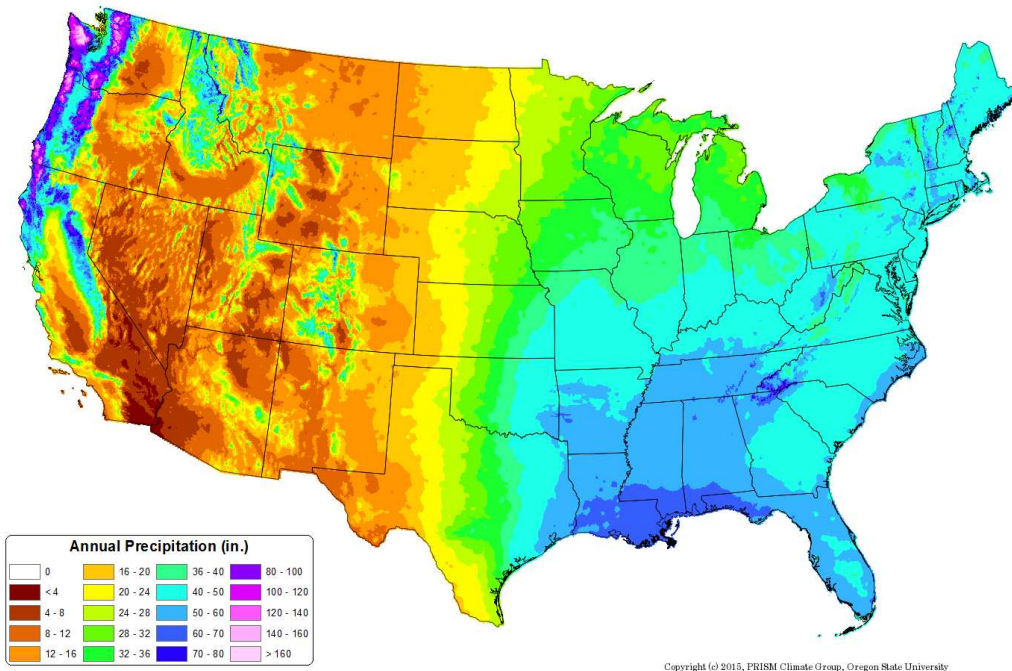


Figure 5. PRISM 30-year (1981-2010) Average Annual Precipitation in Inches (from <http://www.prism.oregonstate.edu/normals>). PRISM.

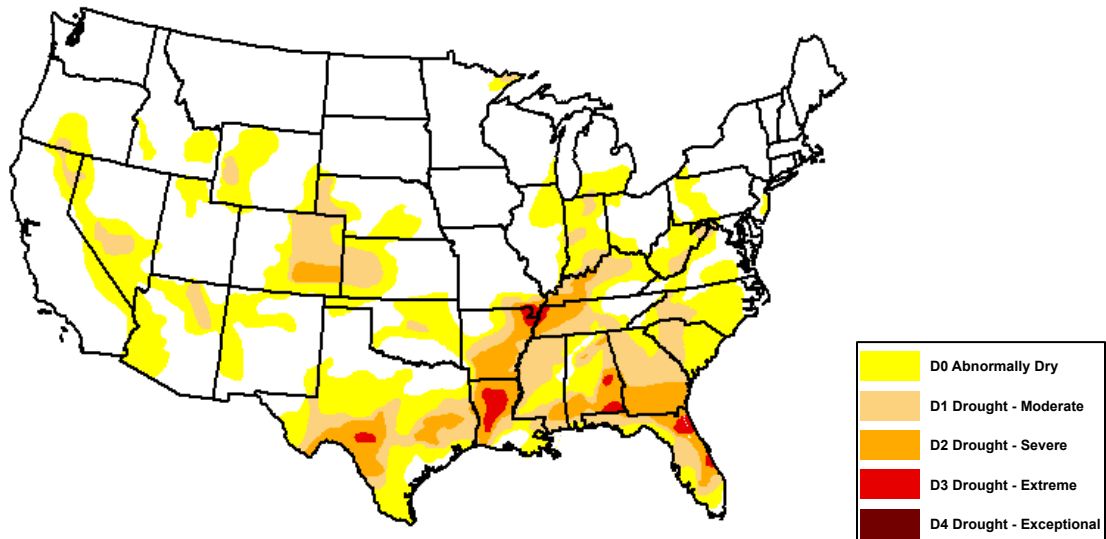


Figure 6. U.S. Drought Monitor Map for November 30th, 2010 <http://droughtmonitor.unl.edu/>. NCDC.

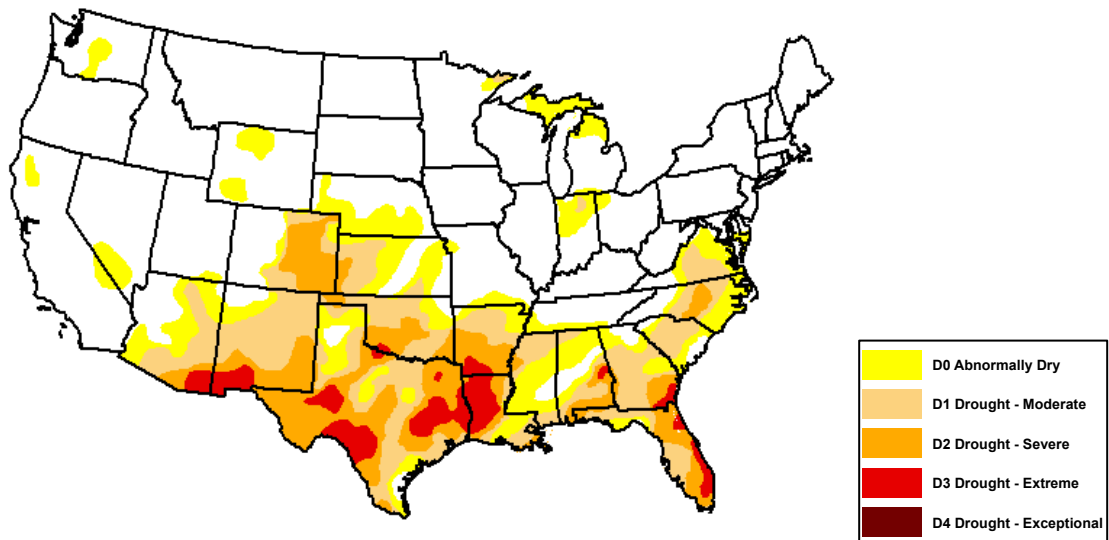


Figure 7. U.S. Drought Monitor Map for March 15th, 2011. <http://droughtmonitor.unl.edu/>. NCDC.

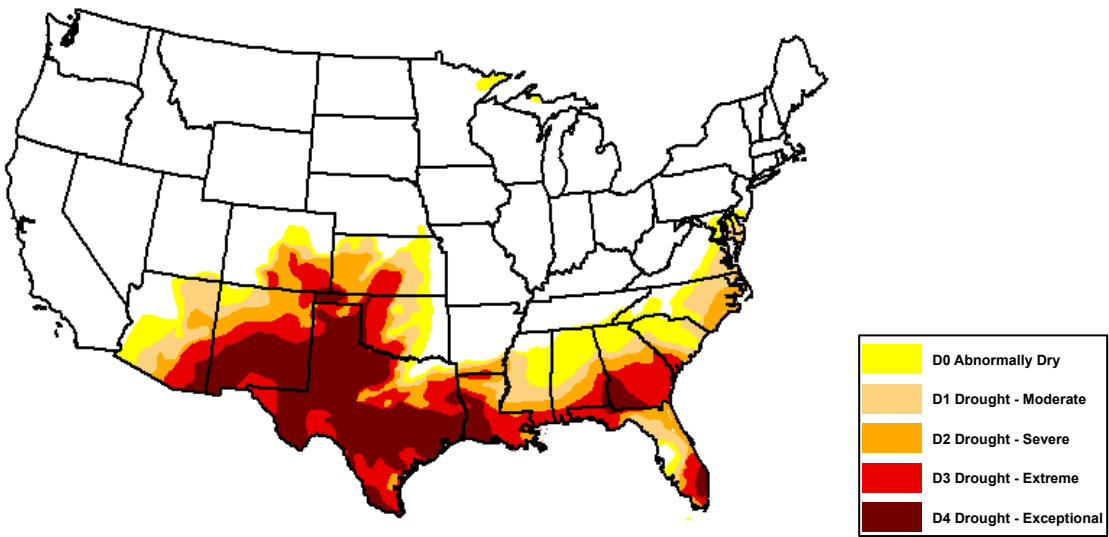


Figure 8. U.S. Drought Monitor Map for June 14th, 2011. <http://droughtmonitor.unl.edu/>. NCDC.

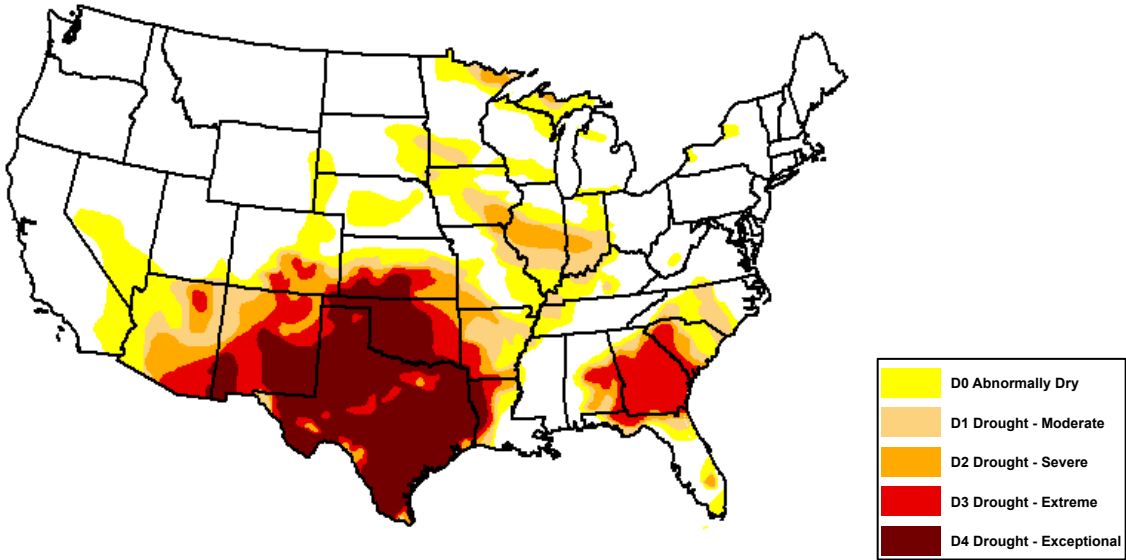


Figure 9. U.S. Drought Monitor Map for September 13th, 2011. <http://droughtmonitor.unl.edu/>. NCDC.

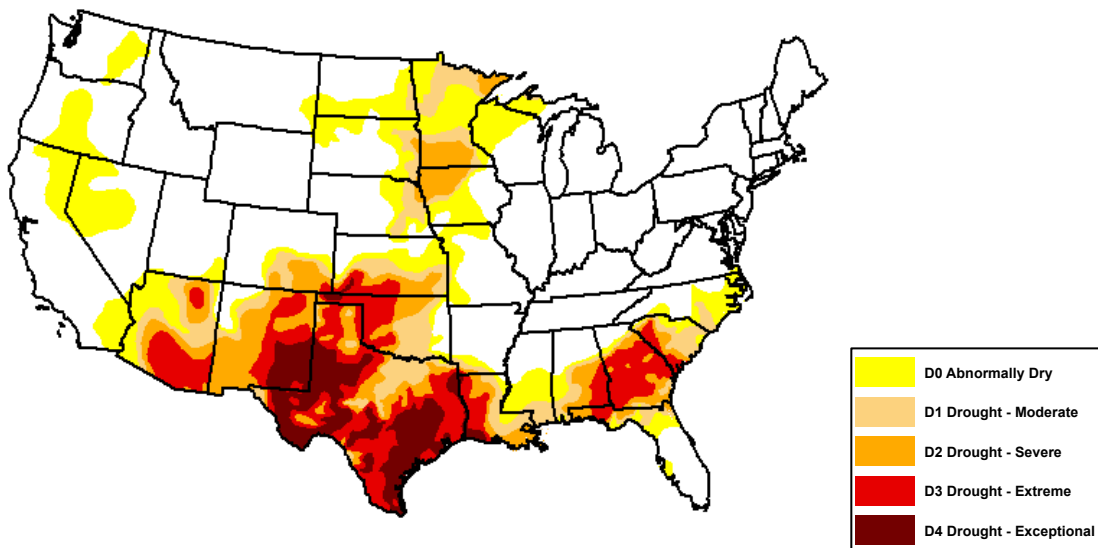


Figure 10. U.S. Drought Monitor Map for December 13th, 2011. <http://droughtmonitor.unl.edu/>. NCDC.

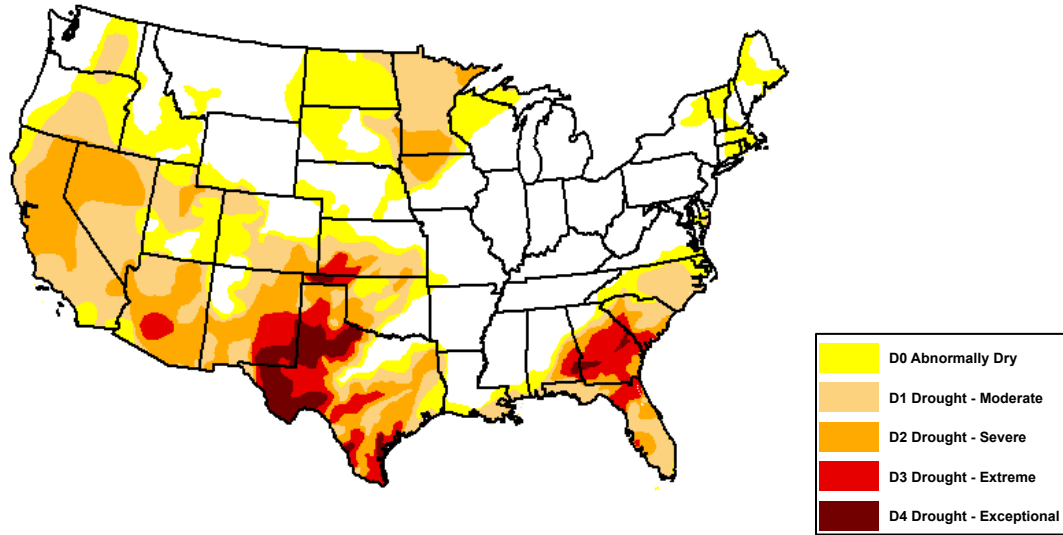


Figure 11. U.S. Drought Monitor Map for March 13th, 2012. <http://droughtmonitor.unl.edu/>. NCDC.

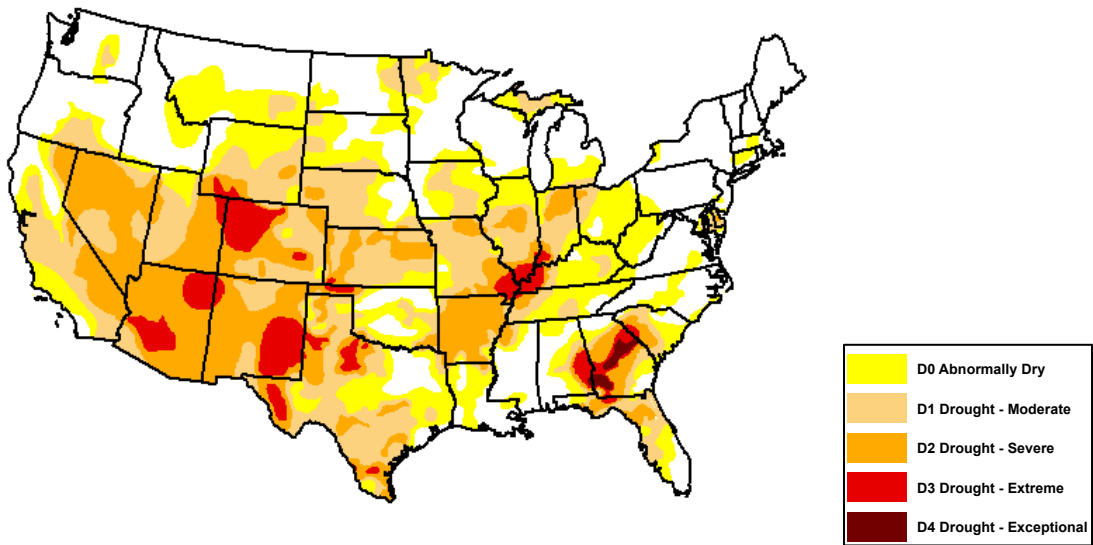


Figure 12. U.S. Drought Monitor Map for June 19th, 2012. <http://droughtmonitor.unl.edu/>. NCDC.

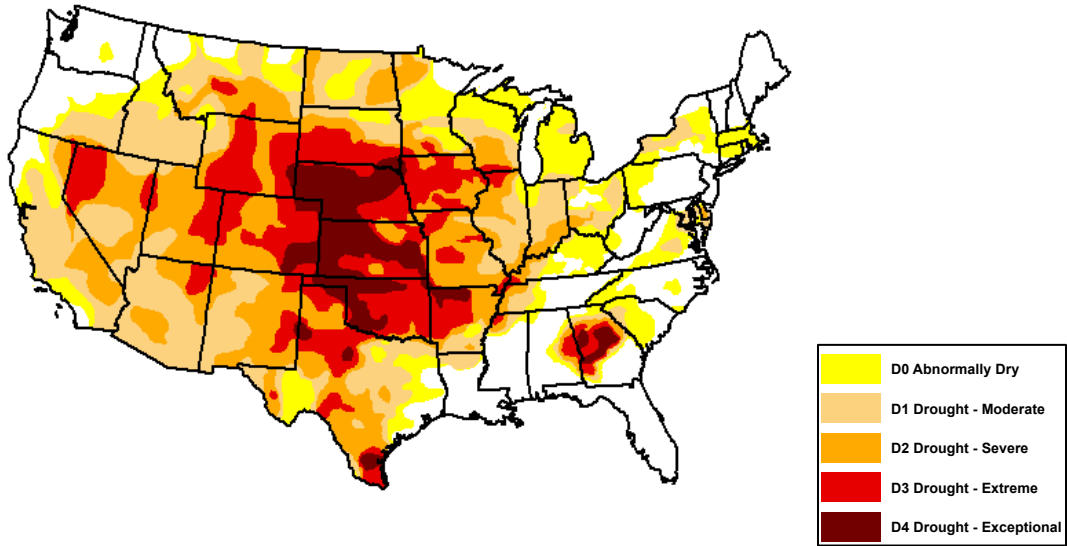


Figure 13. U.S. Drought Monitor Map for September 11th, 2012.
<http://droughtmonitor.unl.edu/>. NCDC.

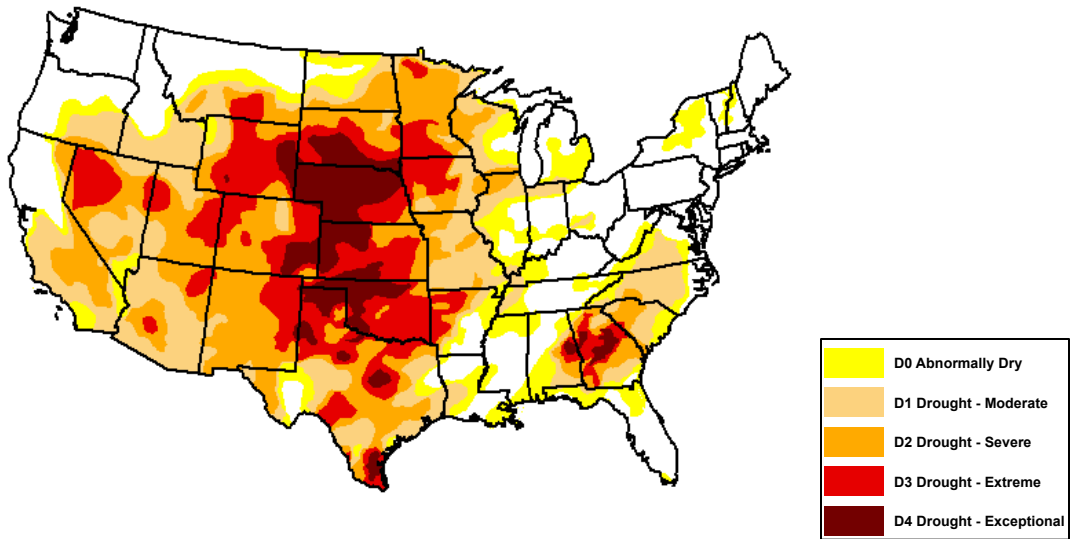


Figure 14. U.S. Drought Monitor Map for December 18th, 2012.
<http://droughtmonitor.unl.edu/>. NCDC.

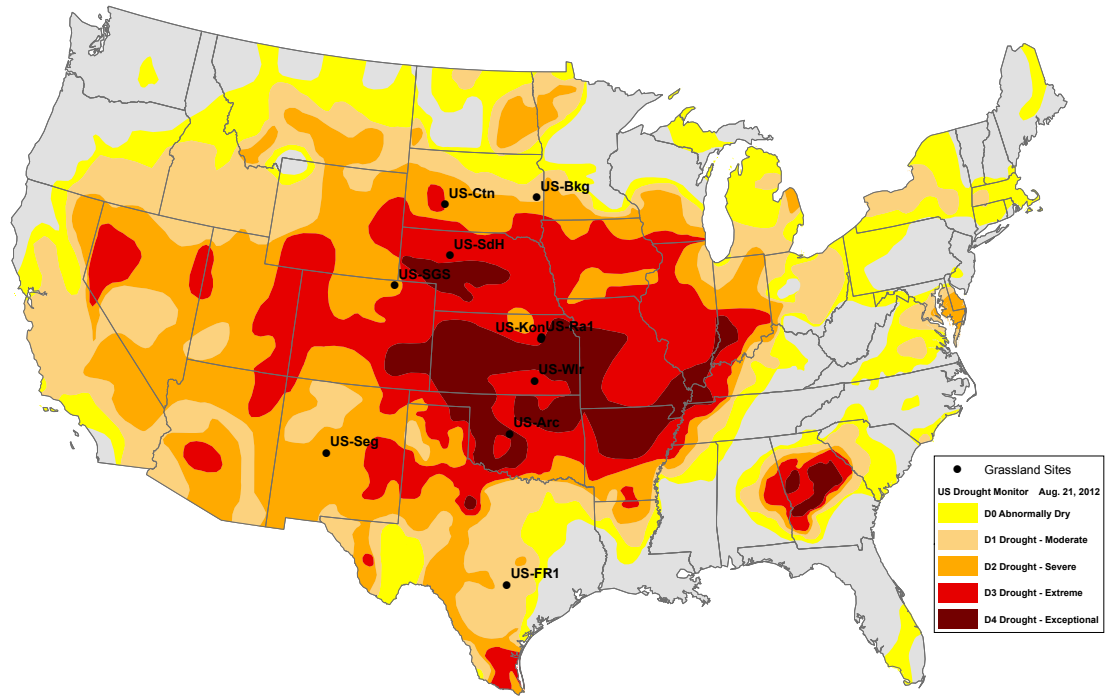


Figure 15. U.S. Drought Monitor Map for August 21st, 2012 with the locations of grassland sites chosen for this study. <http://droughtmonitor.unl.edu/>. NCDC.

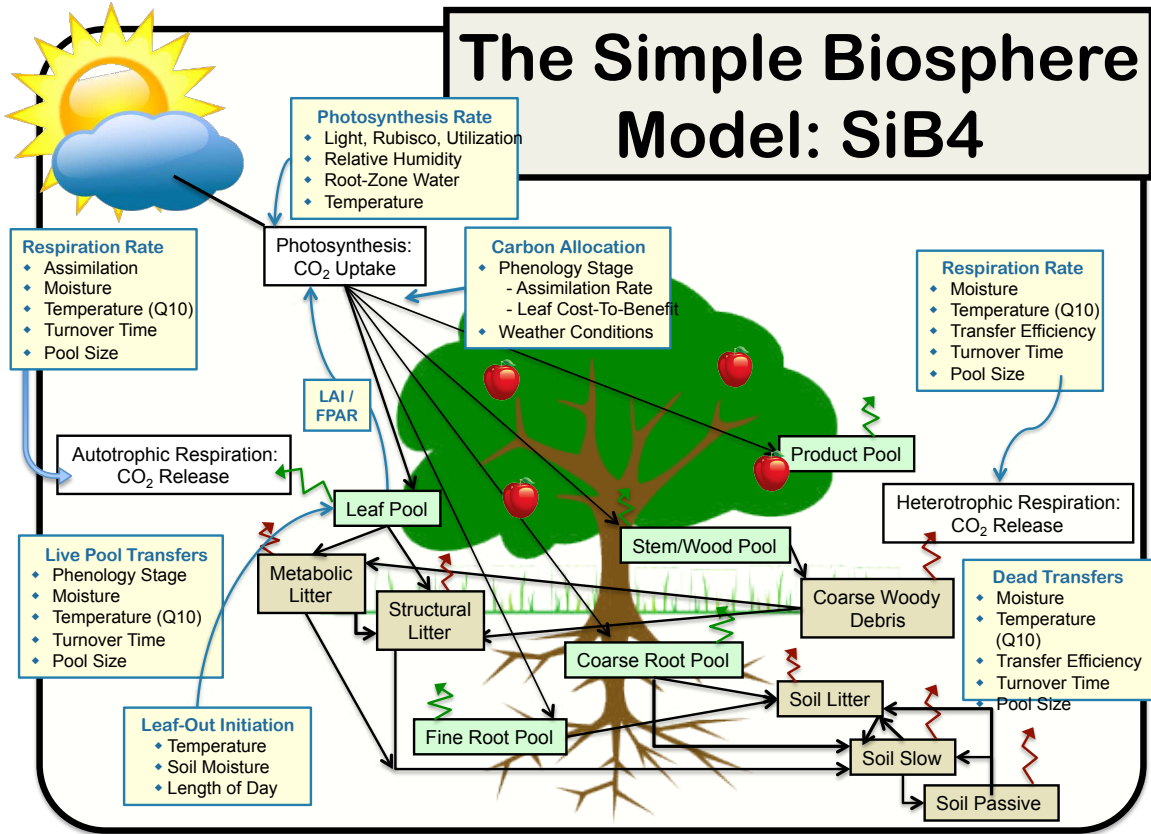


Figure 16. Diagram illustrating how the Simple Biosphere Model Version 4 (SiB4) works.

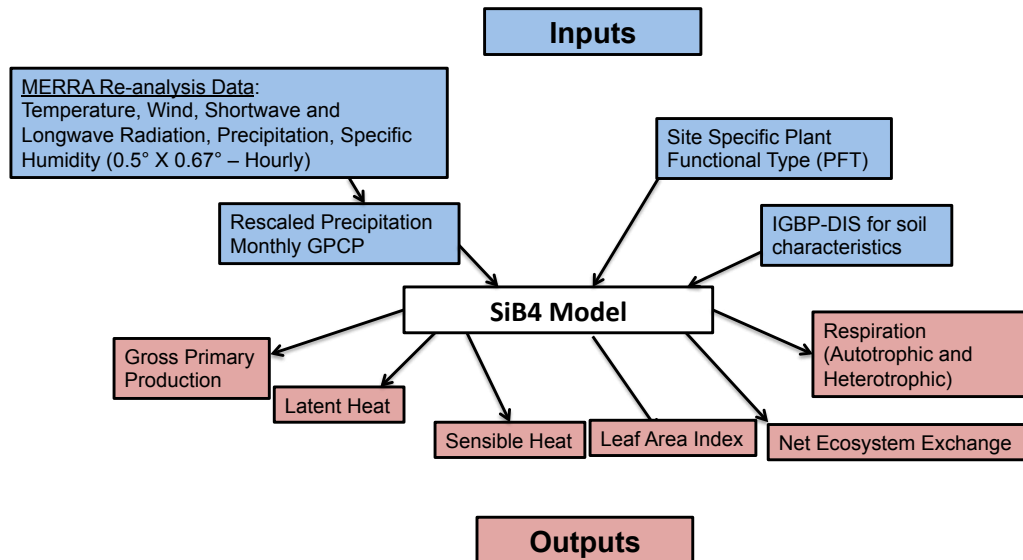


Figure 17. Input Variables (blue boxes) and Output Variables (red boxes) from the Simple Biosphere Model Version 4 (SiB4).



Figure 18. Konza Phenocamera Aug 11, 2012. PhenoCam Network.
<https://phenocam.sr.unh.edu/>. Richardson et al., 2009.



Figure 19. Konza Phenocamera Aug 11, 2015. PhenoCam Network.
<https://phenocam.sr.unh.edu/>. Richardson et al., 2009.

sevilletagrass - NetCam SC_IR - Tue Aug 11 2015 12:30:05 MST - UTC-7
Camera Temperature: 57.0
Exposure: 48



Figure 20. Sevilleta Phenocamera Aug 11, 2015. PhenoCam Network.
<https://phenocam.sr.unh.edu/>. Richardson et al., 2009.

2000–2014 Seasonal Mean Leaf Area Index vs. Annual Mean Precipitation

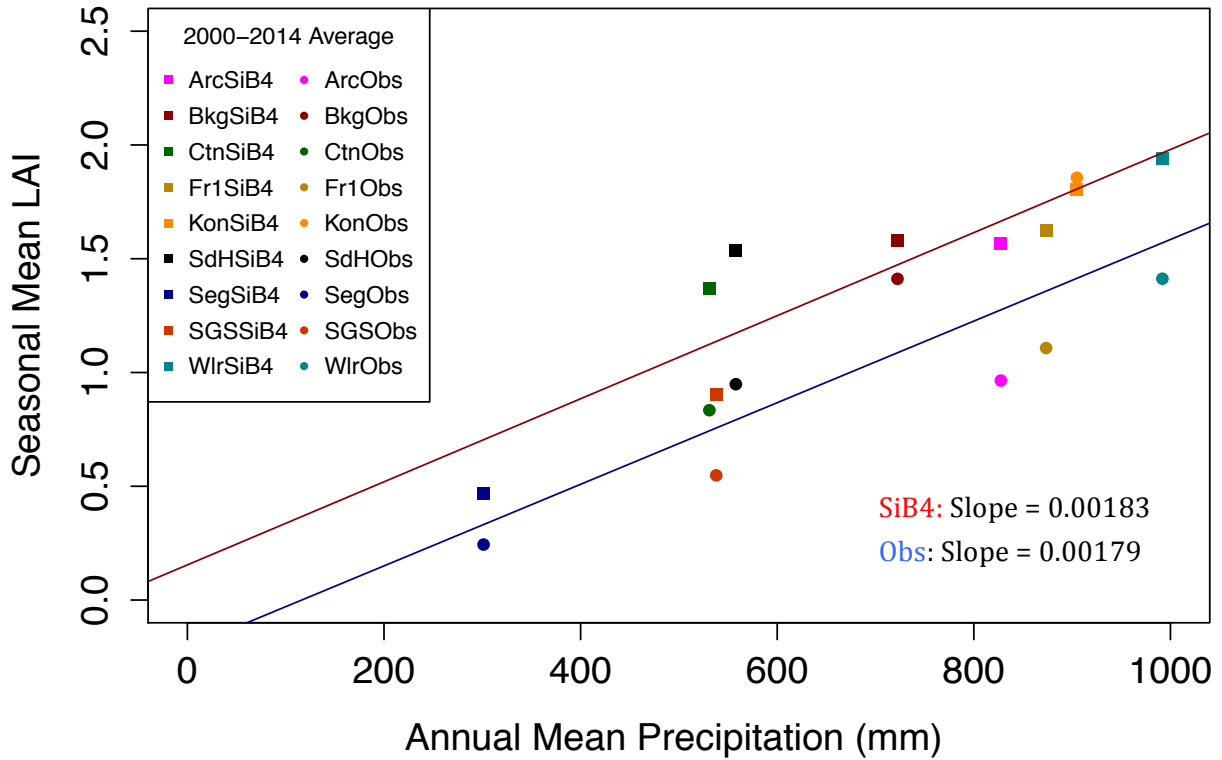


Figure 21. 2000-2014 Seasonal Mean LAI (m^2/m^2) versus Annual Mean Precipitation (mm). Solid squares represent SiB4 values and solid circles represent MODIS/Obs values. SiB, the red line, slope of 0.00183. Obs (MODIS), blue line, slope of 0.00179.

Leaf Area Index and Water Deficit Sevilleta, New Mexico

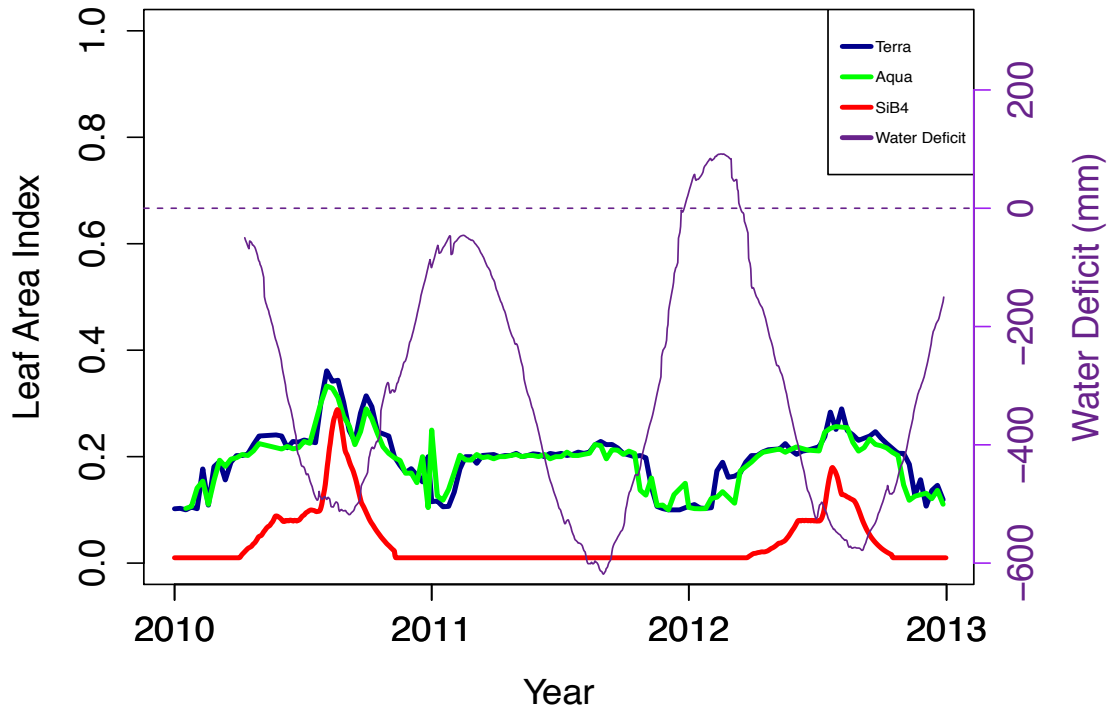


Figure 22. Leaf Area Index (LAI) of the SiB4 (red) and MODIS from Terra (blue) and Aqua (green) for Sevilleta, New Mexico (US-Seg). Purple solid line represents the water deficit values. Plant Functional Type (PFT): 100% C4.

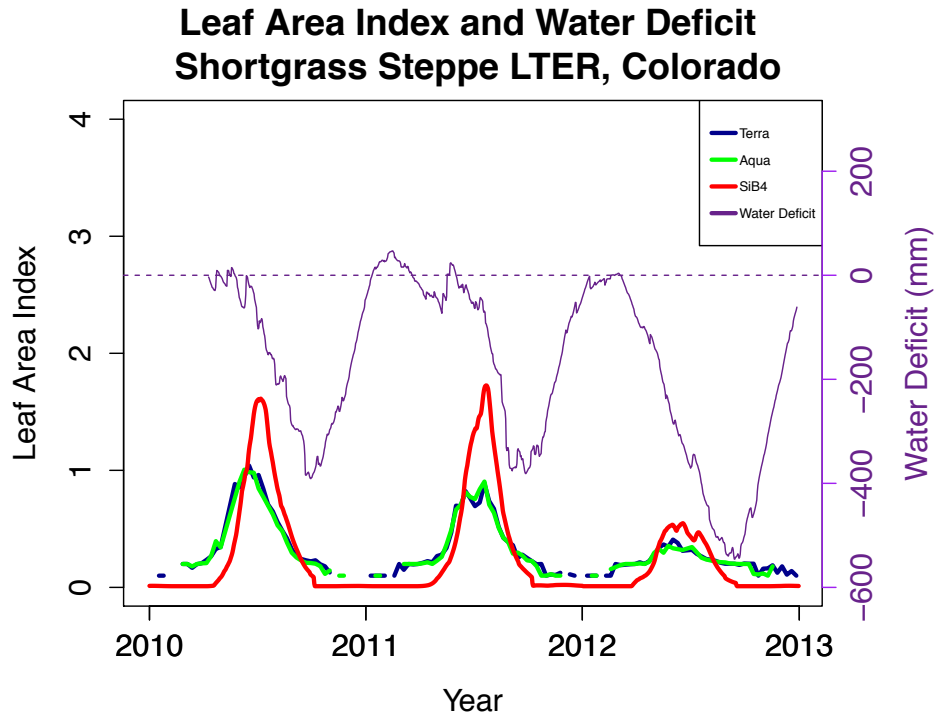


Figure 23. LAI of the SiB4 (red) and MODIS from Terra (blue) and Aqua (green) for Shortgrass Steppe, Colorado (US-SGS). Water Deficit (purple). PFT: 15% C3, 85% C4.

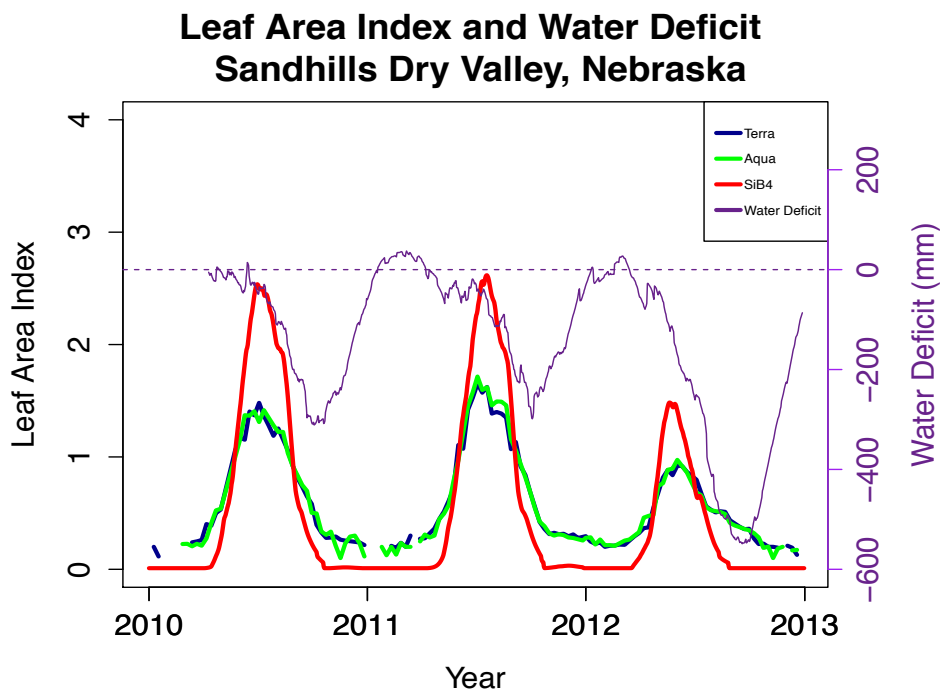


Figure 24. LAI of the SiB4 (red) and MODIS from Terra (blue) and Aqua (green) for Sandhills, Nebraska (US-SdH). Water Deficit (purple). PFT: 40% C3, 60% C4.

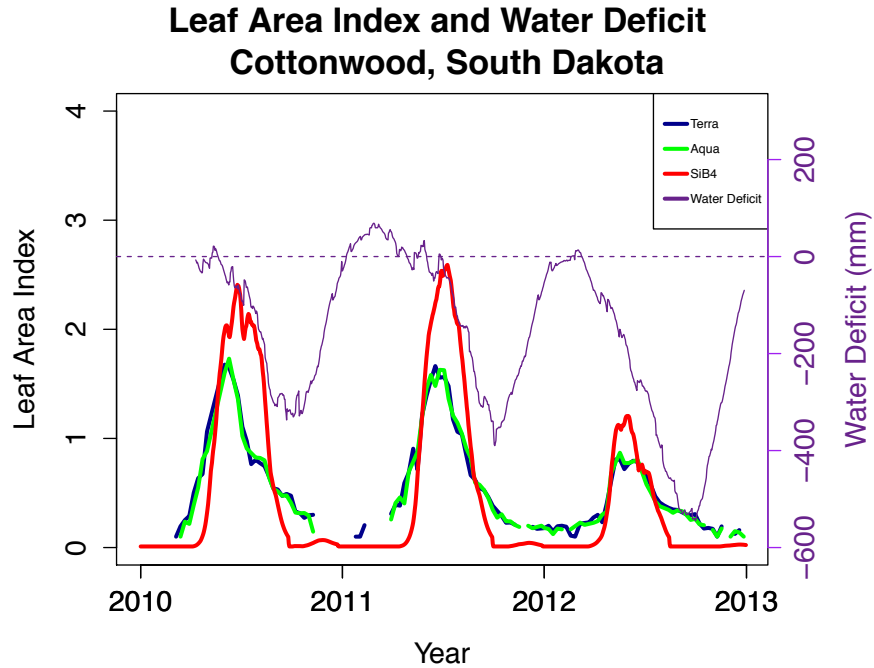


Figure 25. LAI of the SiB4 (red) and MODIS from Terra (blue) and Aqua (green) for Cottonwood, South Dakota (US-Ctn). Water Deficit (purple). PFT: 100% C3.

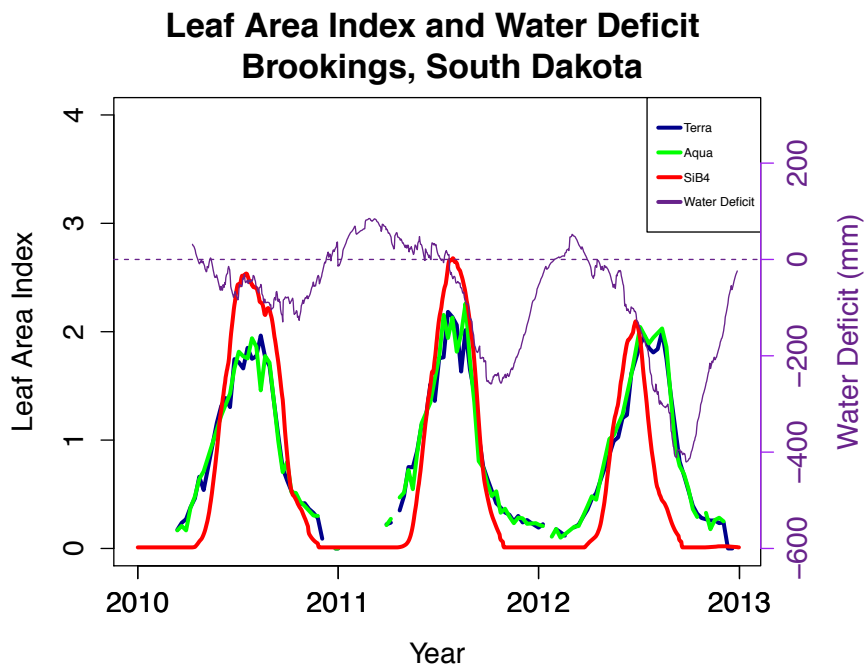


Figure 26. LAI of the SiB4 (red) and MODIS from Terra (blue) and Aqua (green) for Brookings, South Dakota (US-Bkg). Water Deficit (purple). PFT: 15% C3, 85% C4.

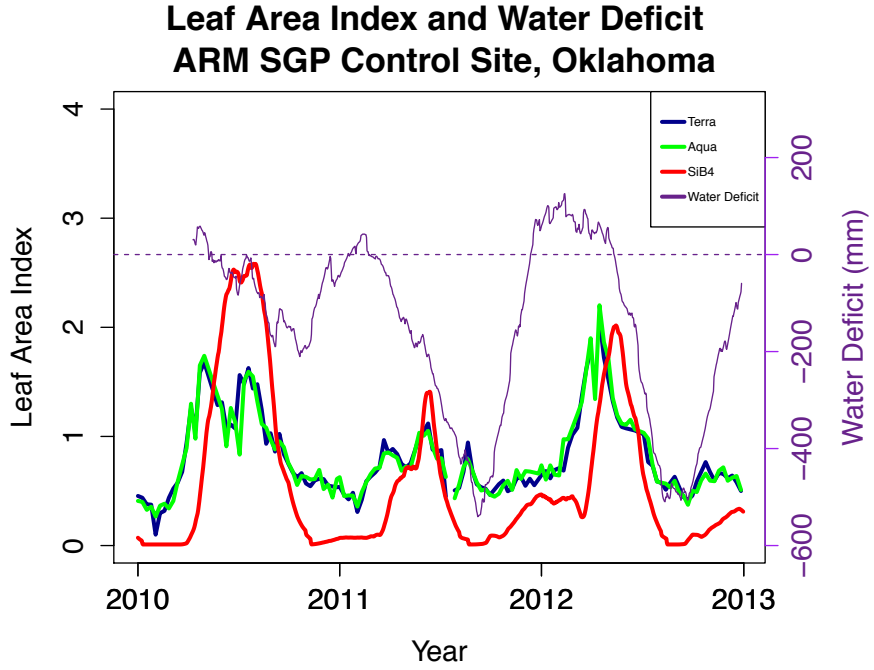


Figure 27. LAI of the SiB4 (red) and MODIS from Terra (blue) and Aqua (green) for ARM Control Site, Oklahoma (US-Arc). Water Deficit (purple). PFT: 40% C3, 60% C4.

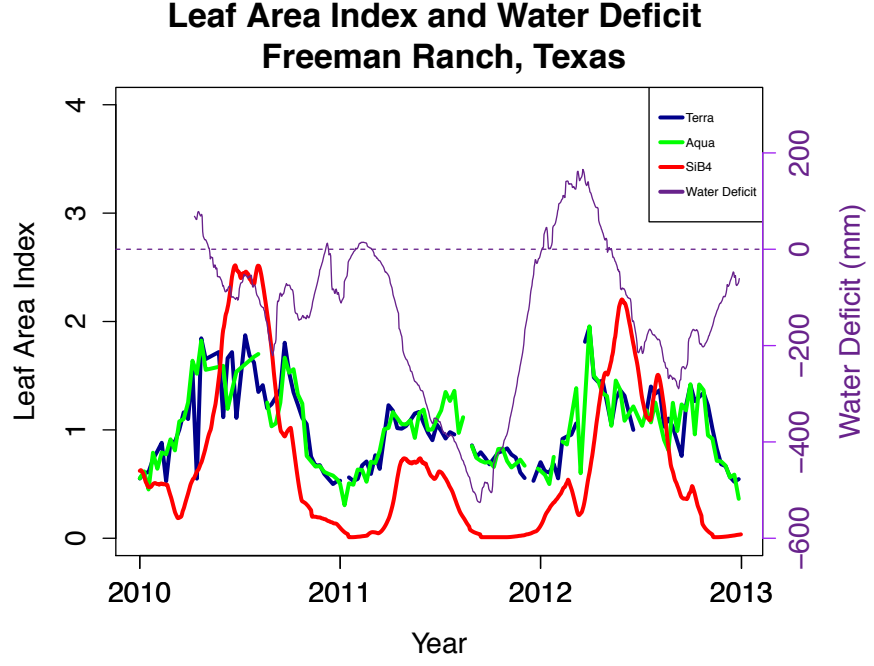


Figure 28. LAI of the SiB4 (red) and MODIS from Terra (blue) and Aqua (green) for Freeman Ranch, Texas (US-Fr1). Water Deficit (purple). PFT: 30% C3, 70% C4.

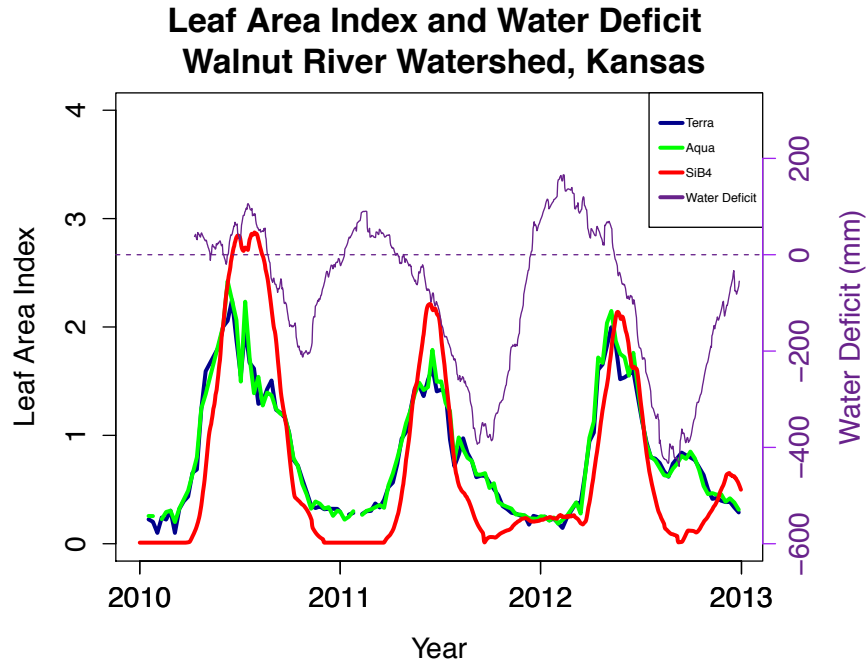


Figure 29. LAI of the SiB4 (red) and MODIS from Terra (blue) and Aqua (green) for Walnut River Watershed, Kansas (US-Wlr). Water Deficit (purple). 35% C3, 65% C4.

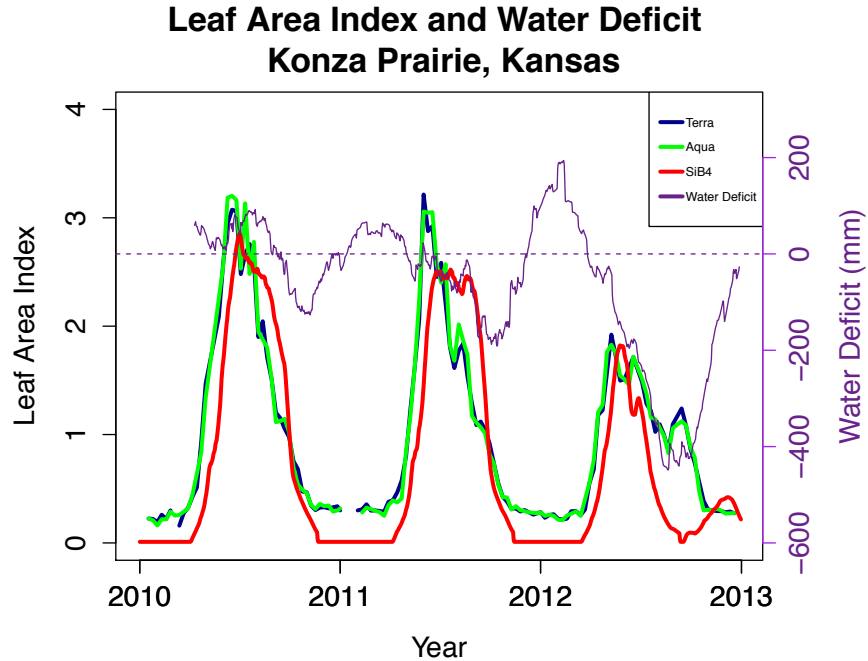


Figure 30. LAI of the SiB4 (red) and MODIS from Terra (blue) and Aqua (green) for Konza Prairie, Kansas (US-Kon). Water Deficit (purple). PFT: 100% C4.

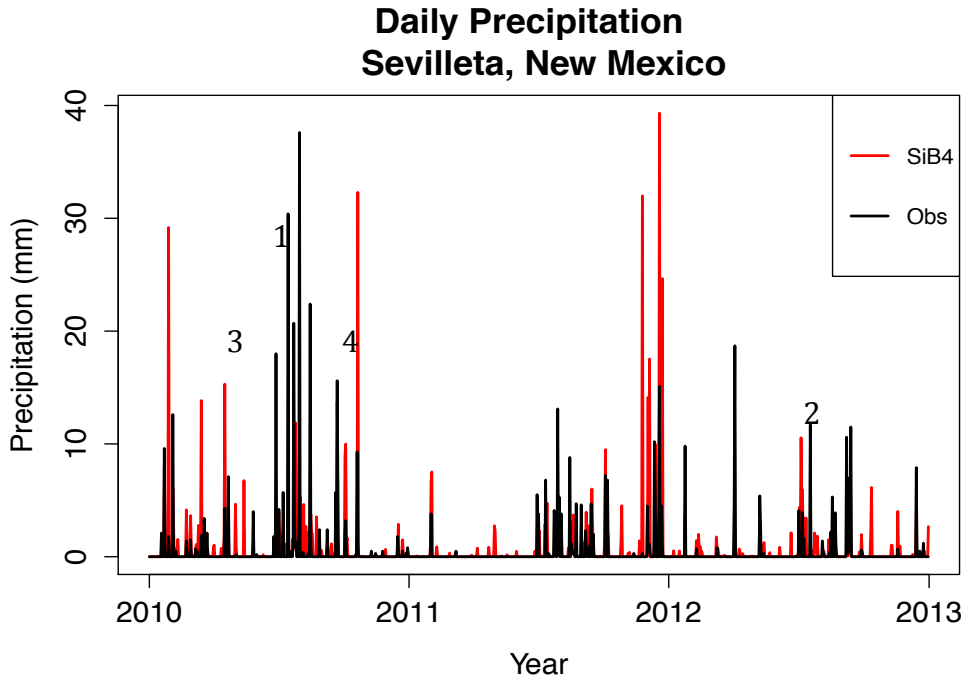


Figure 31. Daily Precipitation in millimeters from 2010-2012 for Sevilleta, New Mexico (US-Seg). Red Lines: MERRA data in SiB4. Black Lines: Rain Gauge Data (USCRN - Diamond et al. 2013).

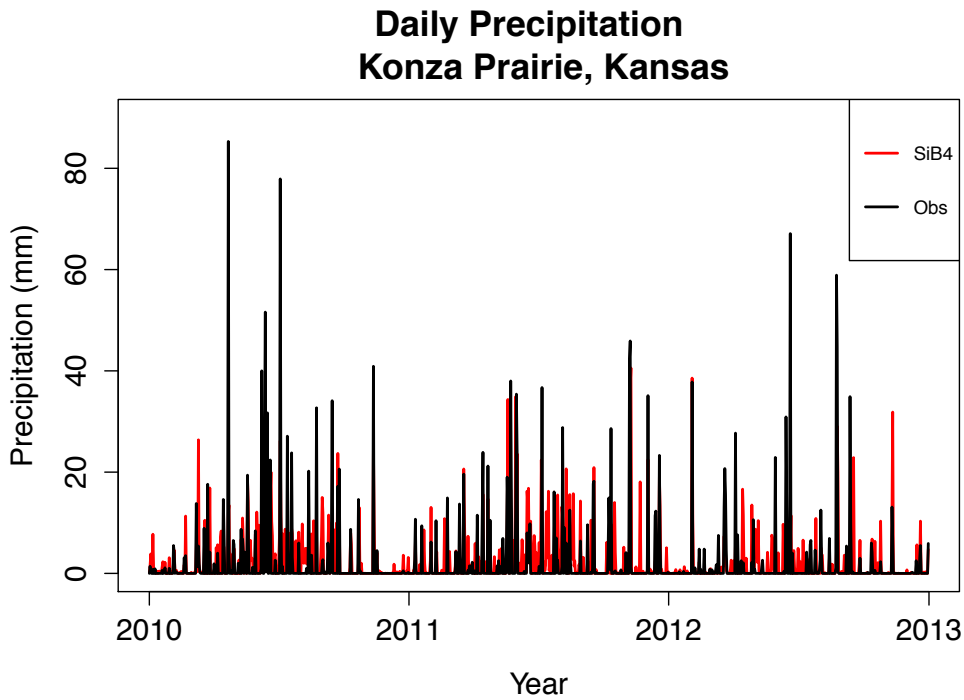


Figure 32. Daily Precipitation in millimeters from 2010-2012 at Konza Prairie, Kansas (US-Kon). Red Lines: MERRA data in SiB4. Black Lines: Rain Gauge Data (USCRN – Diamond et al. 2013).

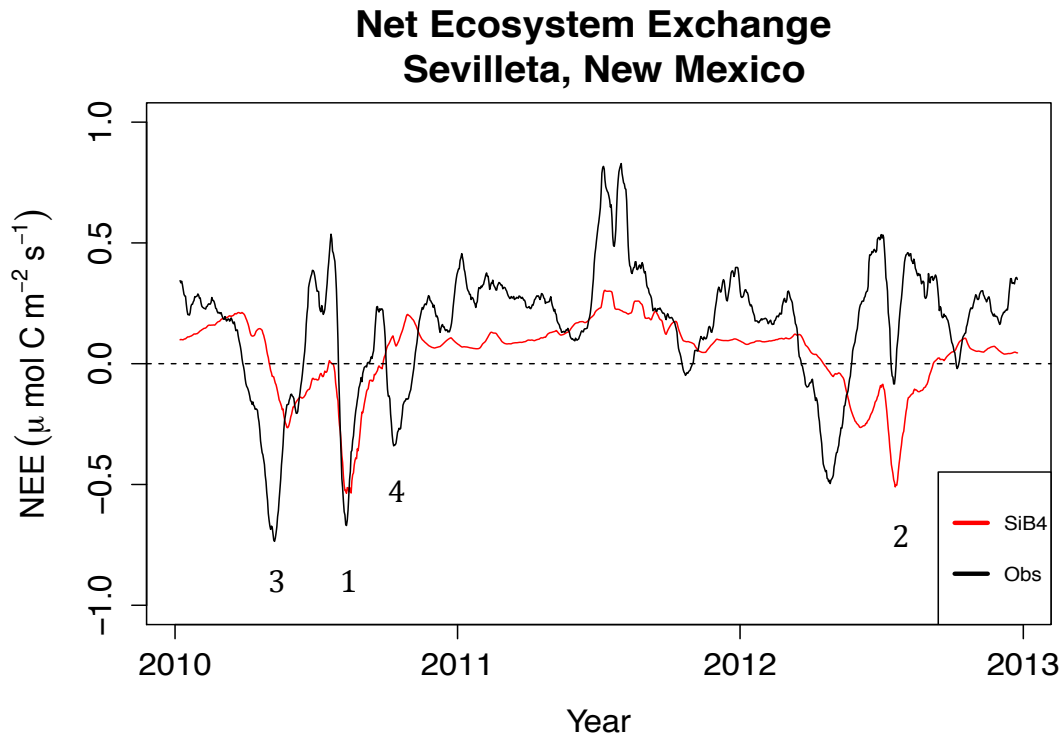


Figure 33. Net Ecosystem Exchange (NEE) at Sevilleta, New Mexico (US-Seg). Red line is from SiB4 and black line from flux tower. #'s represent precipitation events.

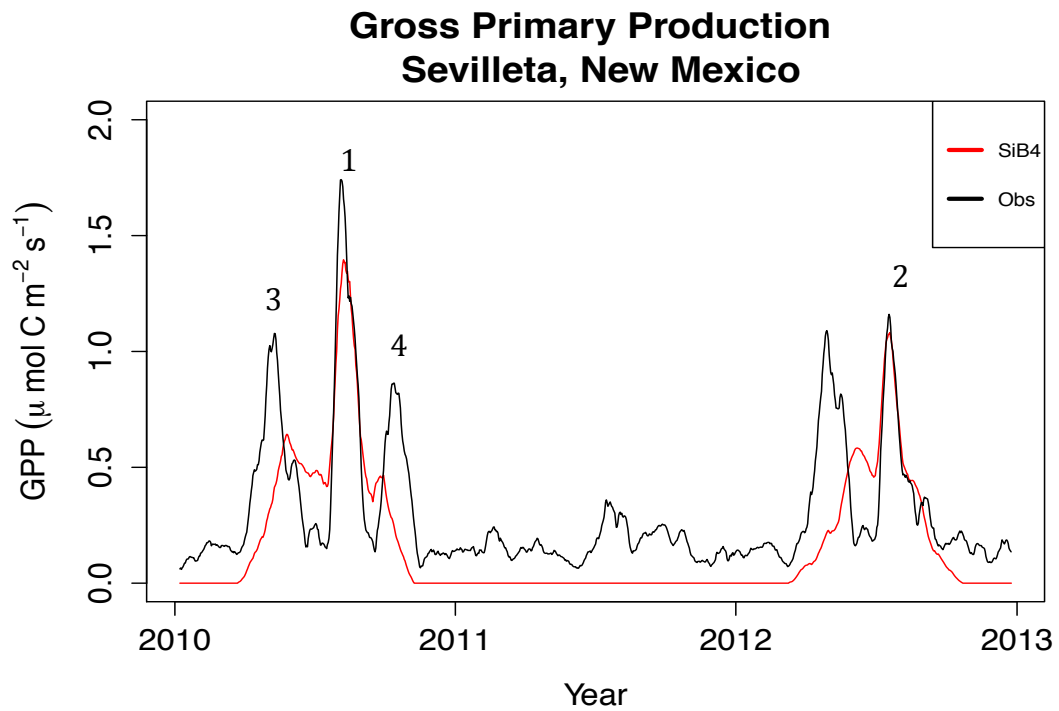


Figure 34. Gross Primary Productivity (GPP) at Sevilleta, New Mexico (US-Seg). Red line is from SiB4 and black line from flux tower. #'s represent precipitation events.

Latent Heat Flux Sevilleta, New Mexico

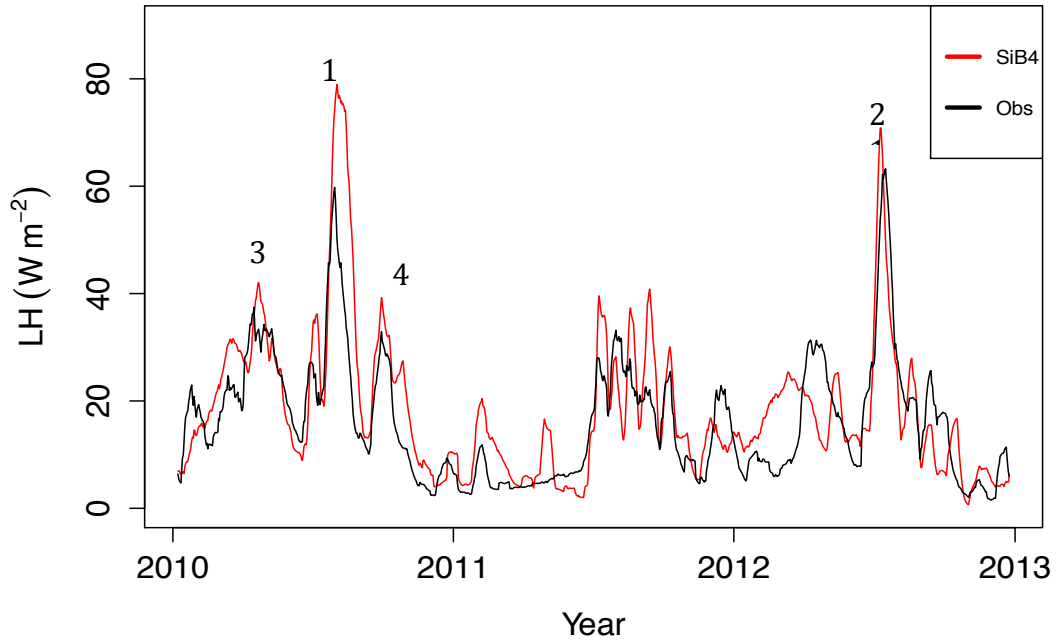


Figure 35. Latent Heat (LH) values at Sevilleta, New Mexico (US-Seg). Red line is from SiB4 and black line from flux tower. #'s represent precipitation events.

Sensible Heat Flux Sevilleta, New Mexico

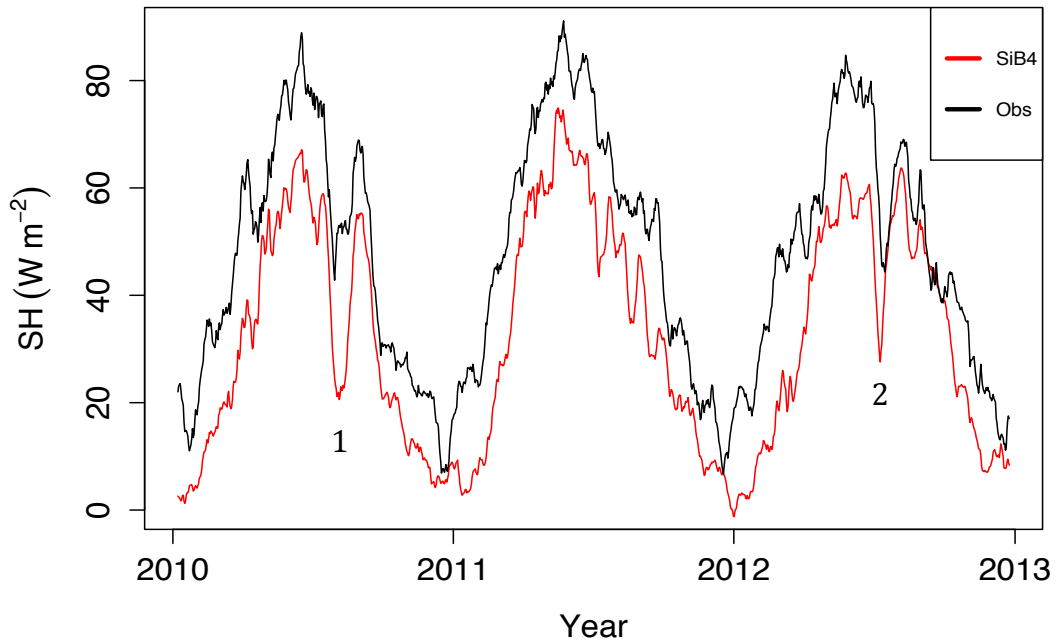


Figure 36. Sensible Heat (SH) values at Sevilleta, New Mexico (US-Seg). Red line is from SiB4 and black line from flux tower. #'s represent precipitation events.

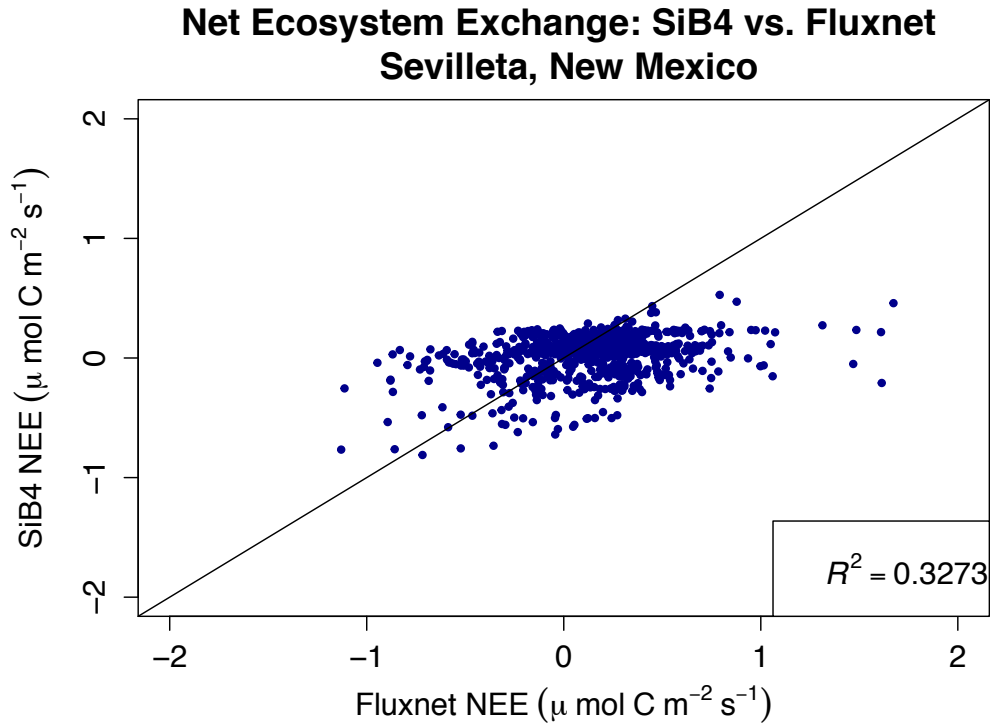


Figure 37. Daily values of Net Ecosystem Exchange (NEE) at Sevilleta, New Mexico. SiB4 (model) versus Fluxnet (observations) from 2010-2012.

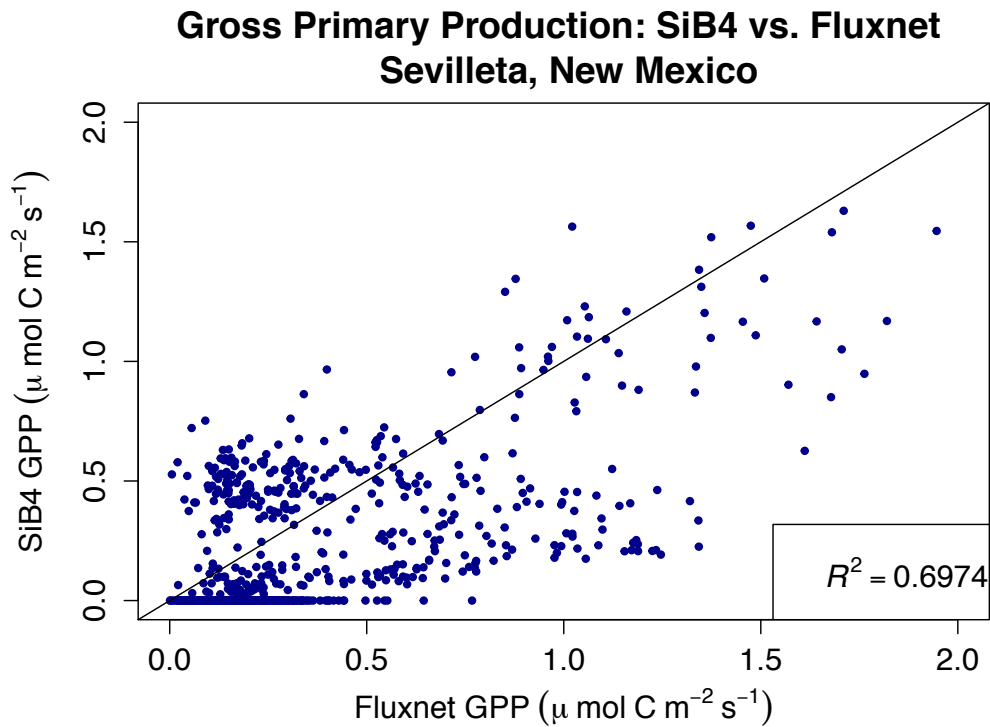


Figure 38. Daily values of Gross Primary Production (GPP) at Sevilleta, New Mexico. SiB4 (model) versus Fluxnet (observations) from 2010-2012.

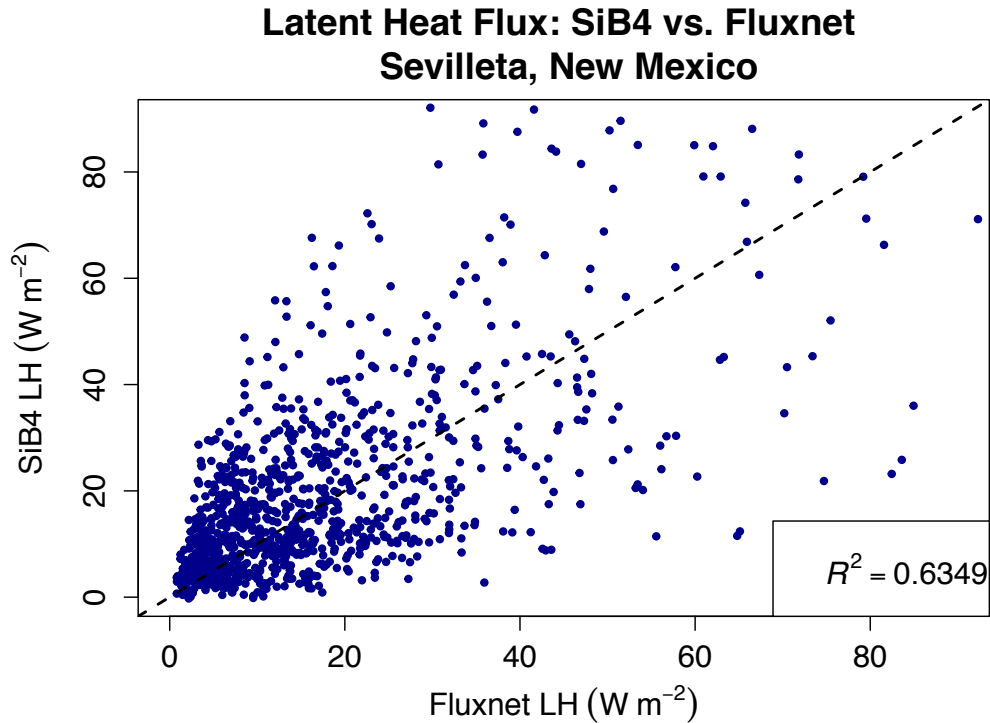


Figure 39. Daily values of Latent Heat (LH) at Sevilleta, New Mexico. SiB4 (model) versus Fluxnet (observations) from 2010-2012.

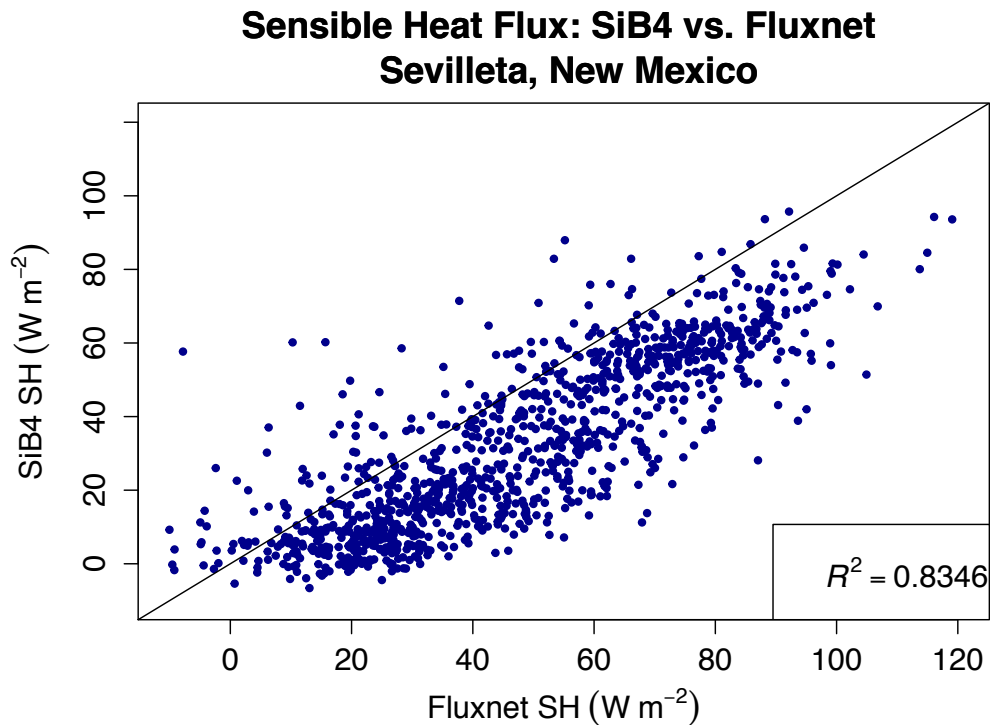


Figure 40. Daily values of Sensible Heat (SH) at Sevilleta, New Mexico. SiB4 (model) versus Fluxnet (observations) from 2010-2012.

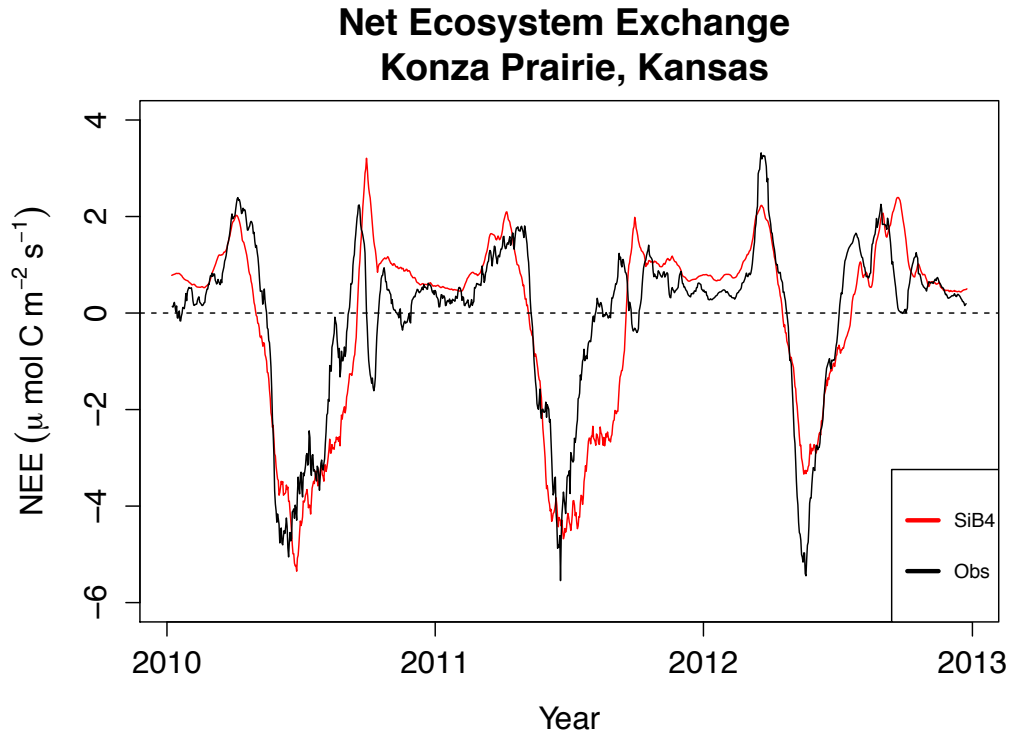


Figure 41. Net Ecosystem Exchange (NEE) values at Konza Prairie, Kansas (US-Kon). Red line is from SiB4 and black line from flux tower.

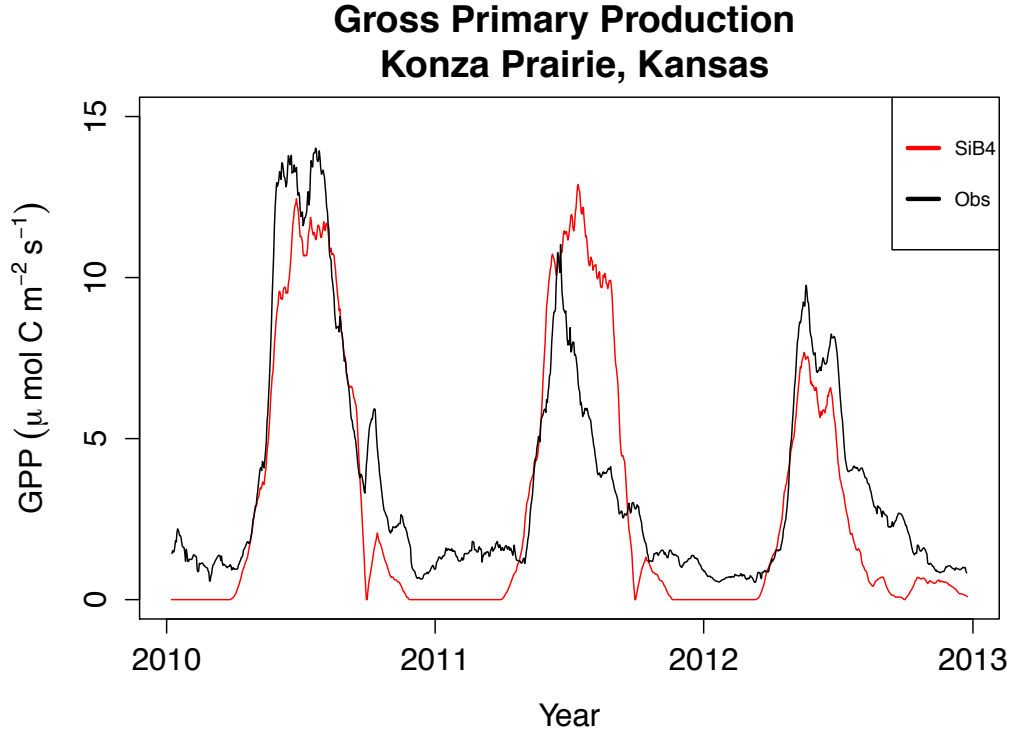


Figure 42. Gross Primary Production (GPP) values at Konza Prairie, Kansas (US-Kon). Red line is from SiB4 and black line from flux tower.

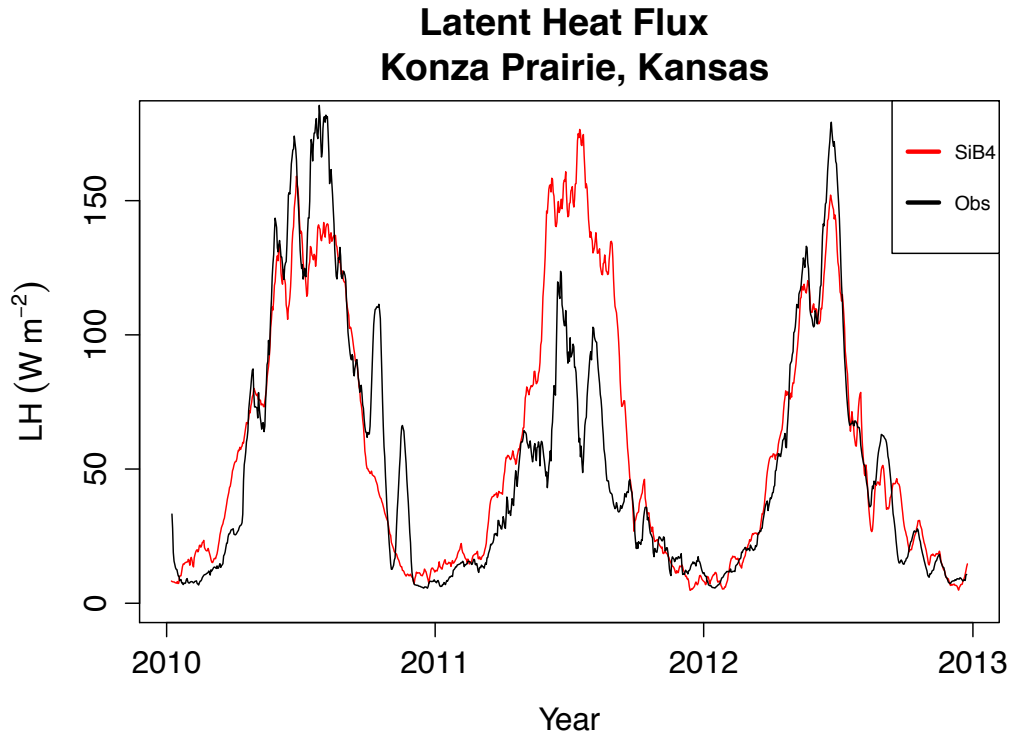


Figure 43. Latent Heat (LH) values at Konza Prairie, Kansas (US-Kon). Red line is from SiB4 and black line from flux tower.

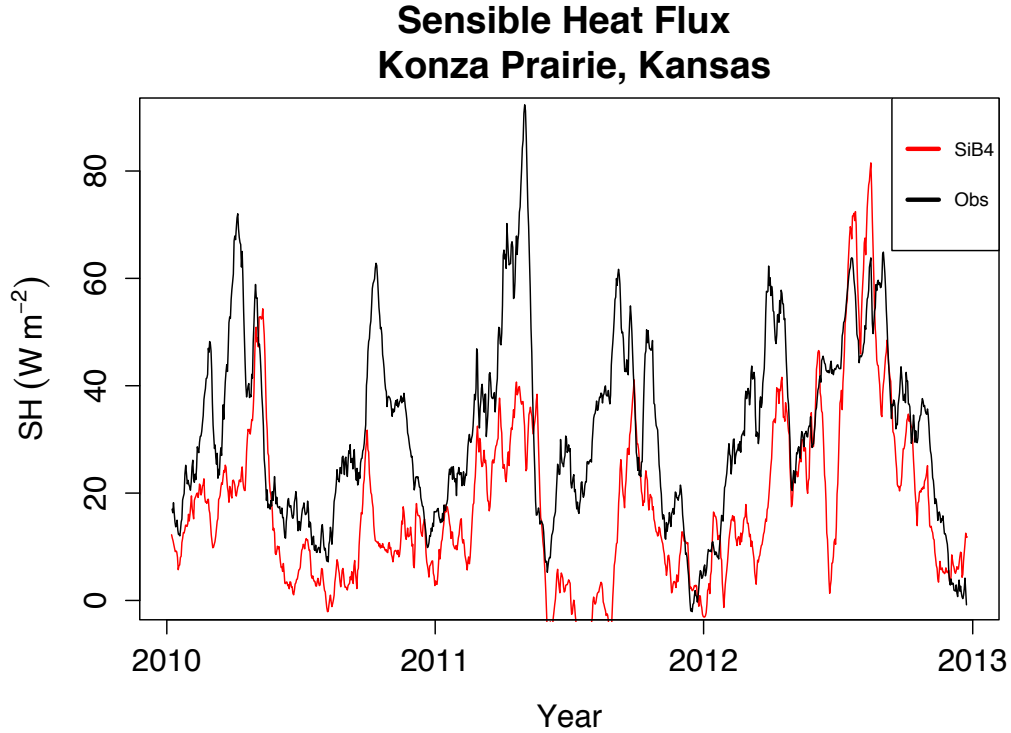


Figure 44. Sensible Heat Flux (SH) values at Konza Prairie, Kansas (US-Kon). Red line is from SiB4 and black line from flux tower.

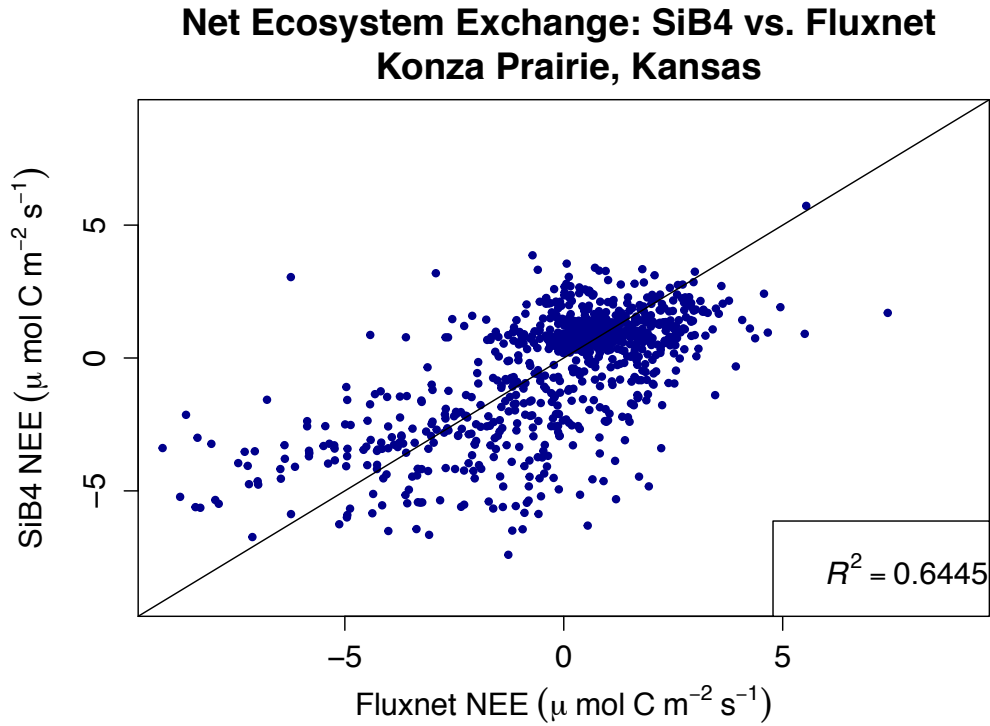


Figure 45. Daily values of Net Ecosystem Exchange (NEE) at Konza Prairie, Kansas. SiB4 (model) versus Fluxnet (observations) from 2010-2012.

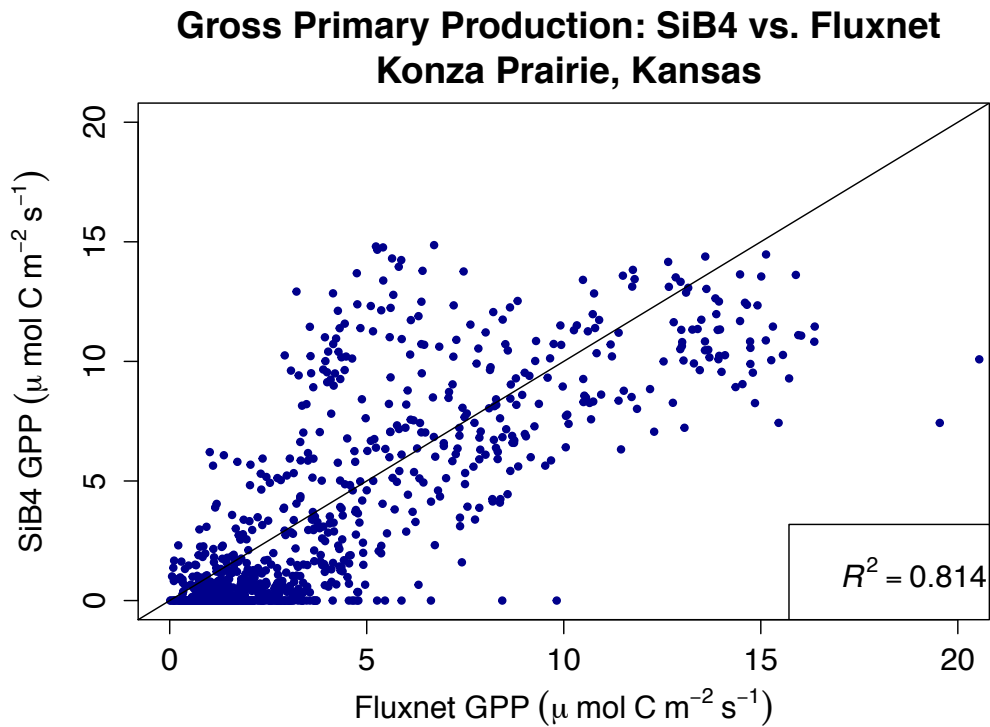


Figure 46. Daily values of Gross Primary Production (GPP) at Konza Prairie, Kansas. SiB4 (model) versus Fluxnet (observations) from 2010-2012.

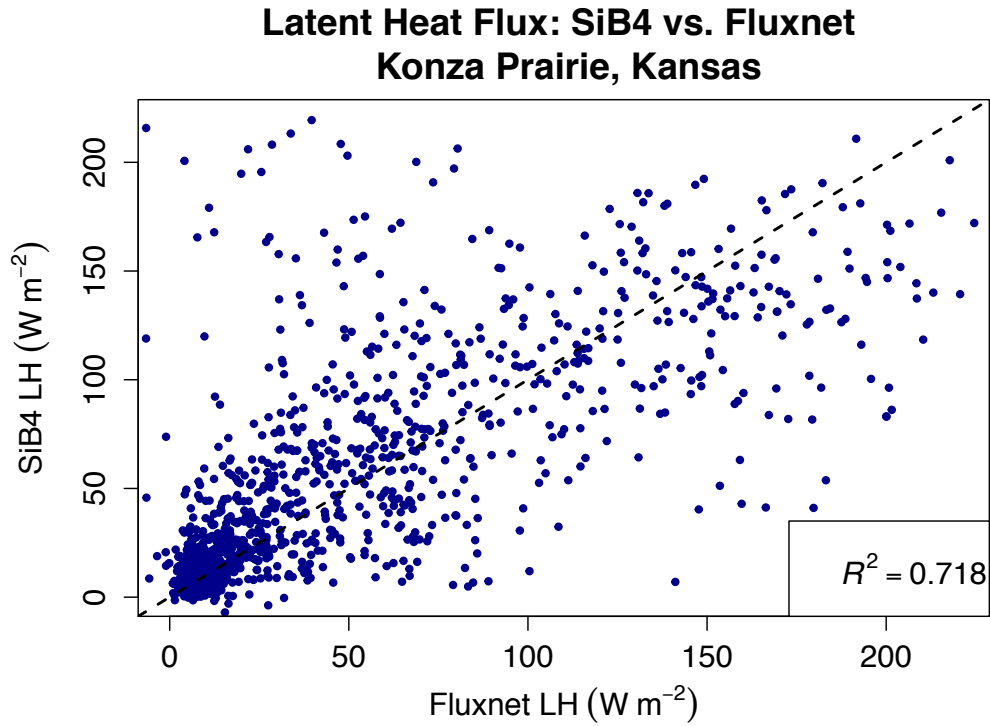


Figure 47. Daily values of Latent Heat (LH) at Konza Prairie, Kansas. SiB4 (model) versus Fluxnet (observations) from 2010-2012.

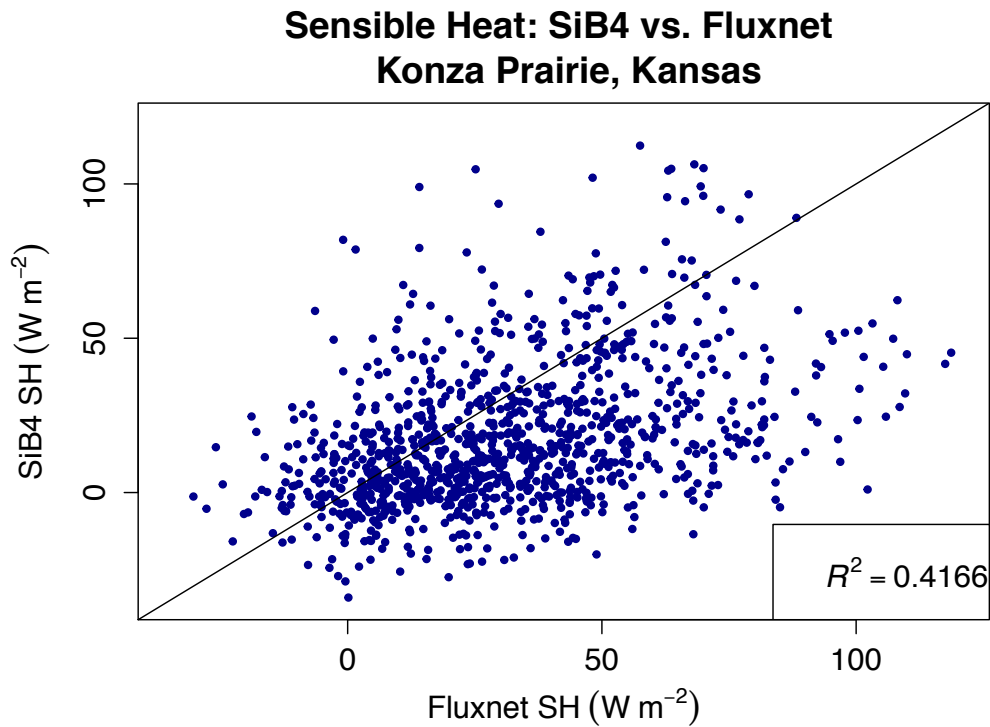


Figure 48. Daily values of Sensible Heat (SH) at Konza Prairie, Kansas. SiB4 (model) versus Fluxnet (observations) from 2010-2012.

Anomalies of Seasonal Mean Leaf Area Index of SiB4 vs. Precipitation Anomaly

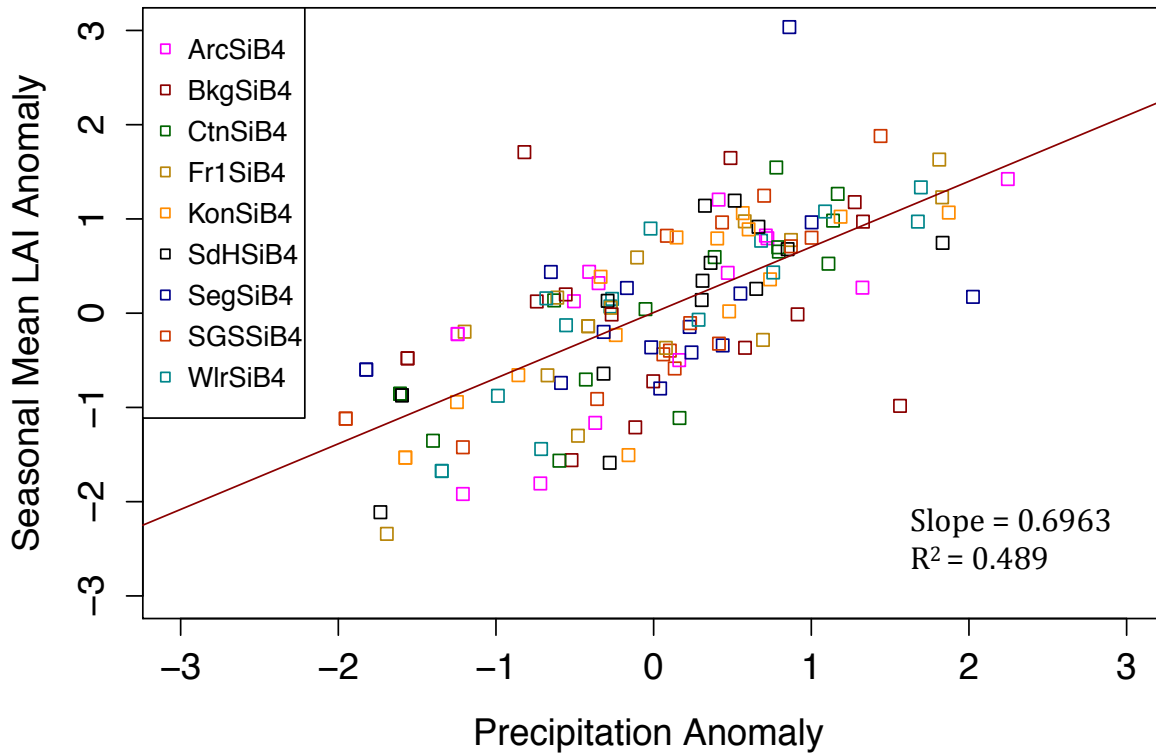


Figure 49. Standardized Anomalies of Seasonal Mean LAI of SiB4 versus the Annual Precipitation Anomaly. Red line is correlation for SiB4. Slope = 0.6963 and $R^2 = 0.489$.

Anomalies of Seasonal Mean Leaf Area Index of Obs vs. Precipitation Anomaly

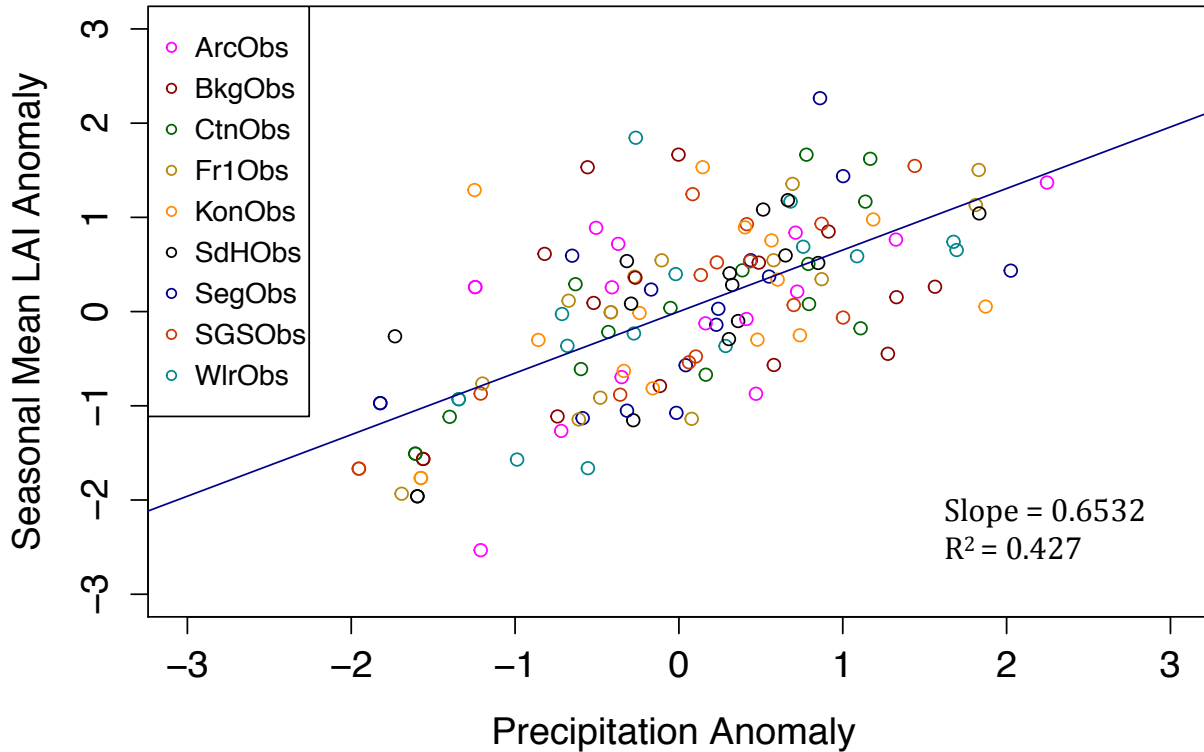


Figure 50. Standardized Anomalies of Seasonal Mean LAI of Observations (MODIS) versus the Annual Precipitation Anomaly. Red line is the correlation for SiB4. Slope = 0.6963 and $R^2 = 0.489$.

2010 Seasonal Mean Leaf Area Index Anomaly vs. Annual Mean Precipitation Anomaly

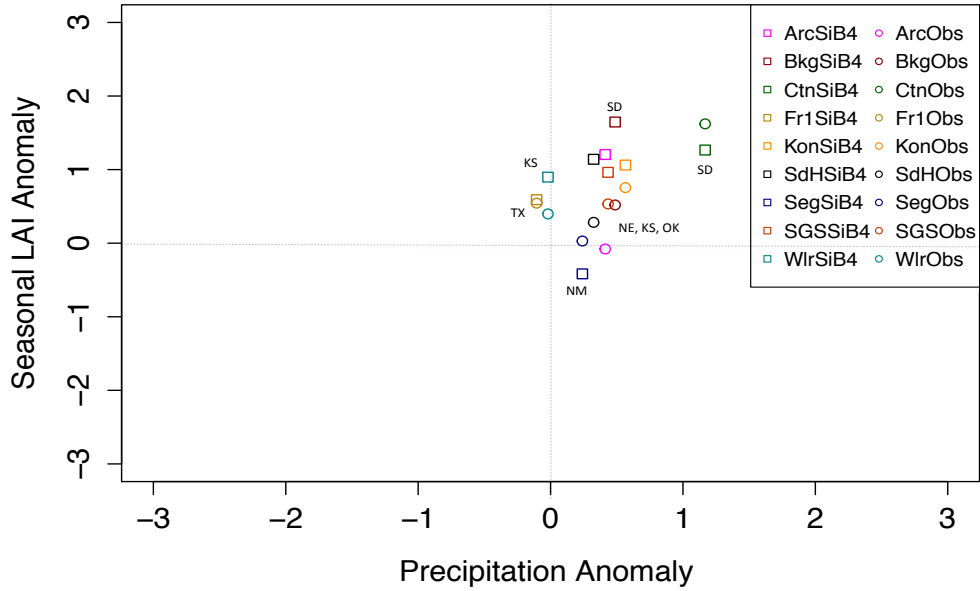


Figure 51. 2010 Standardized Anomalies of Seasonal Mean LAI of SiB4 and MODIS (Obs) versus the Annual Precipitation Anomaly. States listed for each site.

2011 Seasonal Mean Leaf Area Index Anomaly vs. Annual Mean Precipitation Anomaly

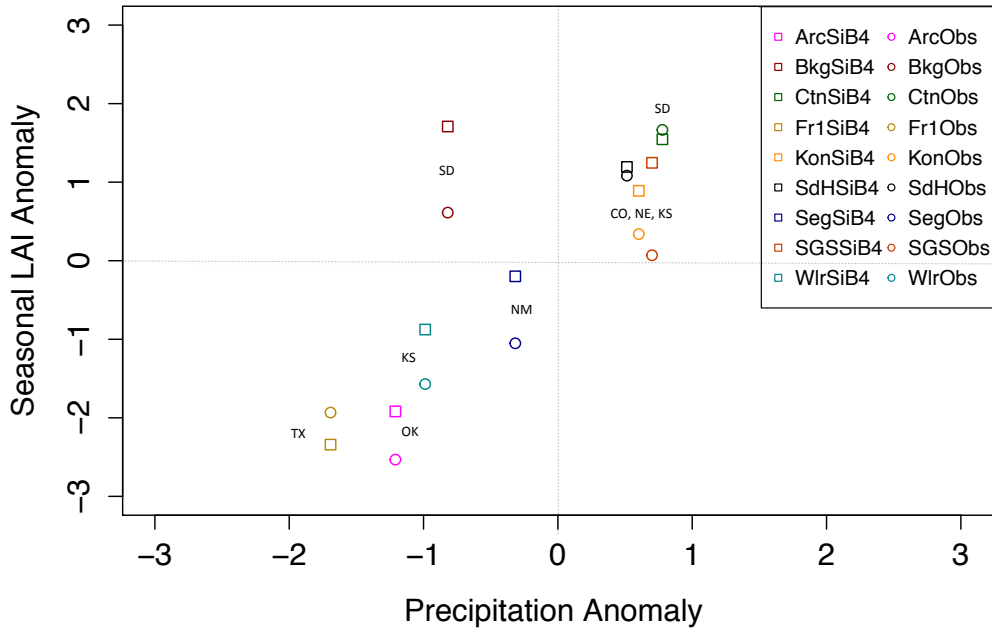


Figure 52. 2011 Standardized Anomalies of Seasonal Mean LAI of SiB4 and MODIS (Obs) versus the Annual Precipitation Anomaly. States listed for each site.

2012 Seasonal Mean Leaf Area Index Anomaly vs. Annual Mean Precipitation Anomaly

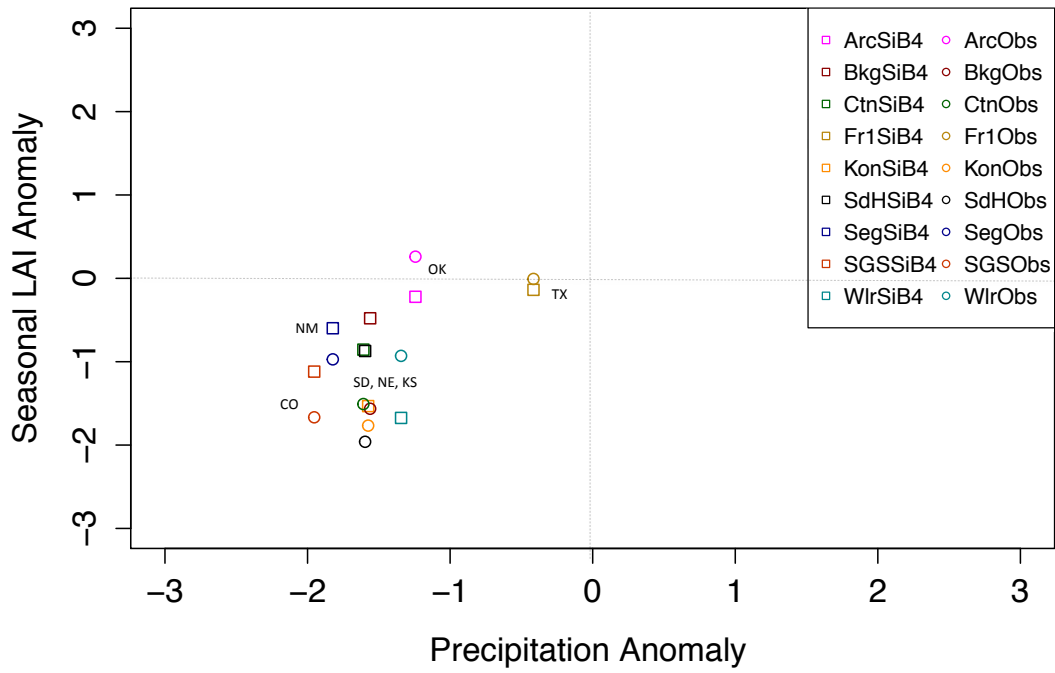


Figure 53. 2012 Standardized Anomalies of Seasonal Mean LAI of SiB4 and MODIS (Obs) versus the Annual Precipitation Anomaly. States listed for each site.

2000–2014 Seasonal Mean Leaf Area Index vs. Annual Mean Precipitation

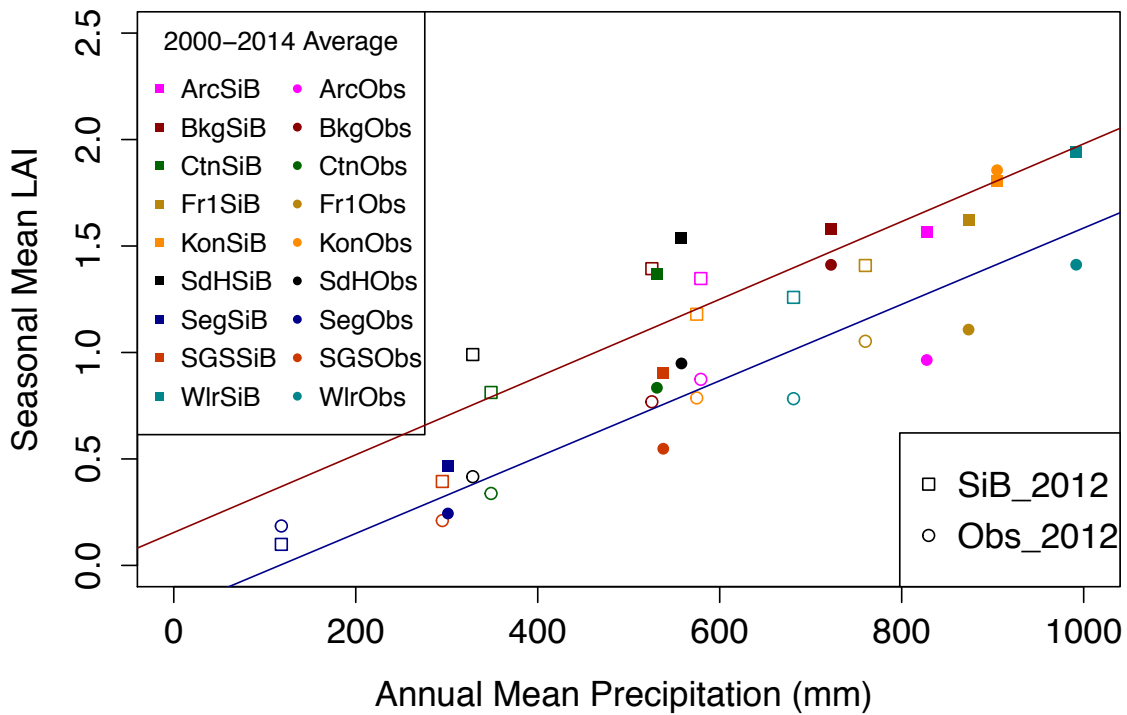


Figure 54. 2000-2014 Seasonal Mean LAI (m^2/m^2) versus Annual Mean Precipitation (mm). Solid squares represent SiB4 values (15-year mean) and solid circles represent MODIS/Obs values (15-year mean). Open squares represent the 2012 SiB4 values while the open circles represent the obs values in 2012.

REFERENCES

- Albertson, F.W., J.E. Weaver, 1944. Nature and degree of recovery of grassland from the great drought of 1933 to 1940. *Ecol Monogr* 14:393–479
- Ashouri H, Sorooshian S, Hsu K, Bosilovich MG, Lee J, Wehner MF, 2015. Evaluation of NASA's MERRA precipitation product in reproducing the observed trend and distribution of extreme precipitation events in the United States. *J Hydrometeor* 17:693–711. doi:10.1175/JHM-D-15-0097.1
- Bagne, K.; Ford, P.; Reeves, M. , 2012. Grasslands. U.S. Department of Agriculture, Forest Service, Climate Change Resource Center. www.fs.usda.gov/ccrc/topics/grasslands/
- Baker, I.T., A.S. Denning, N. Hanan, L. Prihodko, P.-L. Vidale, K. Davis and P. Bakwin, 2003. Simulated and observed fluxes of sensible and latent heat and CO₂ at the WLEF-TV Tower using SiB2.5. *Global Change Biology*, 9, 1262-1277.
- Baldocchi, D.D. and K.B. Wilson, 2001. Modeling CO₂ and water vapor exchange of a temperate broadleaved forest across hourly to decadal time scales, *Ecol. Model.*, 142, 155-184.
- Baldocchi, D.D., 2003. Assessing the eddy covariance technique for evaluating carbon dioxide exchange rates of ecosystems: past, present and future. *Global Change Biol.* 9, 479–492
- Blair, J.M., Nippert, J.B., Briggs, J.M., 2013, October. Grassland ecology. In: Monson, R. (Ed.), *The Plant Sciences – Ecology and the Environment*. Springer Verlag, Berlin, Heidelberg, pp. 1–28
- Chazdon, R.L., 1978. Ecological aspects of the distribution of C-4 grasses in selected habitats of costa-rica. *Biotropica*, 10, 265–269.
- Clapp, R. B., and G. M. Hornberger, 1978. Empirical equations for some soil hydraulic properties, *Water Resour. Res.*, 14(4), 601–604, doi:10.1029/WR014i004p00601.
- Collatz, G.J., J.T. Ball, C. Grivet, and J.A. Berry , 1991. Physiological and environmental regulation of stomatal conductance, photosynthesis and transpiration: a model that includes a laminar boundary layer, *Agric. For. Meteorol.*, 54, 107-136.
- Collatz, G.J., M. Ribas-Carbo, and J.A. Berry, 1992. Coupled photosynthesis-stomatal conductance model for leaves of C₄ plants, *Aust. J. Plant Physiol.*, 19, 519-538.
- Collatz, G.J., Berry, J.A. & Clark, J.S., 1998. Effects of climate and atmospheric CO₂ partial pressure on the global distribution of C₄ grasses: present, past, and future. *Oecologia*, 114, 441–454.
- Craine JM, Wedin DA, Chapin FS III, Reich PB, 2002. Relationship between the structure of root systems and resource use for 11 North American grassland plants. *Plant Ecol* 165:85–100
- Craine J.M., J.B. Nippert JB, A.J. Elmore, A.M. Skibbe, S.L. Hutchinson, and N.A. Brunsell, 2012. Timing of climate variability and grassland productivity. *Proceedings of the National Academy of Sciences*, doi: 10.1073/pnas.1118438109

- Davidson A. and F. Csillag F, 2003. A comparison of three approaches for predicting C4 species cover of northern mixed grass prairie. *Remote Sensing of Environment*, 86,70–82.
- Denning, A.S., J.G. Collatz, C. Zhang, D.A. Randall, J.A. Berry, P.J. Sellers, G.D. Colello, and D.A. Dazlich, 1996. Simulations of terrestrial carbon metabolism and atmospheric CO₂ in a general circulation model. Part 1: Surface carbon fluxes, *Tellus*, 48B, 521-542.
- Diamond, H.J., T.R. Karl, M.A. Palecki, C.B. Baker, J.E. Bell, R.D. Leeper, D.R. Easterling, J.H. Lawrimore, T.P. Meyers, M.R. Helfert, G. Goodge, and P.W. Thorne, 2013. U.S. Climate Reference Network after one decade of operations: Status and assessment. *Bull. Am. Meteorol. Soc.* doi:10.1175/BAMS-D-12–00170.
- Donohue, R. J., Roderick, M. L., McVicar, T. R. & Farquhar, G. D. , 2013. CO₂ fertilisation has increased maximum foliage cover across the globe’s warm, arid environments. *Geophys. Res. Lett.* 40, 3031–3035
- Farquhar, G. D., S. V. Caemmerer, and J. A. Berry, 1980. A biochemical model of photosynthetic CO₂ assimilation in leaves of C3 species, *Planta*, 149, 78–90, doi:10.1007/BF00386231
- Global Soil Data Task Group, 2000. Global Gridded Surfaces of Selected Soil Characteristics (IGBP-DIS). [Global Gridded Surfaces of Selected Soil Characteristics (International Geosphere-Biosphere Programme - Data and Information System)]. Data set. Available on-line [<http://www.daac.ornl.gov>] from Oak Ridge National Laboratory Distributed Active Archive Center, Oak Ridge, Tennessee, U.S.A. doi:10.3334/ORNLDAAC/569.
- Haynes, K.D., I.T. Baker, A.S. Denning, R. Stockli, K. Schaefer, E.Y. Lokupitiya, and J.M. Haynes, 2016. Unifying Heterogeneous Land Fluxes, Ecosystem Carbon Pools, and Dynamic Prognostic Phenology in the Simple Biosphere Model (SiB4): Part I. Methodology, *Journal of Advances in Modeling Earth Systems*, in preparation
- Hoerling, M., J. Eischeid, A. Kumar, R. Leung, A. Mariotti, K. Mo, S. Schubert, and R. Seager, 2013. Causes and Predictability of the 2012 Great Plains Drought. *Bull. Amer. Meteor. Soc.*, in press.
- Hsu, J.S., J. Powell, and P.B. Adler, 2012, Sensitivity of mean annual primary production to precipitation, *Glob. Change Biol.*, 18, 2246-2255
- Huffman, G. J., R. F. Adler, M. Morrissey, D. Bolvin, S. Curtis, R. Joyce, B. McGavock, and J. Susskind, 2001: Global precipitation at one-degree daily resolution from multisatellite observations, *J. Hydrometeor.*, 2, 36-50.
- Huntzinger, D. N., et al., 2013. The North American Carbon Program Multi-Scale Synthesis and Terrestrial Model Intercomparison Project—Part 1: Overview and experimental design, *Geosci. Model Dev.*, 6,2121–2133, doi:10.5194/gmd-6-2121-2013.
- Huxman, T. E., et al. 2004. Convergence across biomes to a common rain-use efficiency. *Nature* 429:651–654.
- IPCC, 2013: Summary for Policymakers. In: *Climate Change 2013: The Physical Science Basis. Contribution of Working Group I to the Fifth Assessment Report of the Intergovernmental Panel on Climate Change* [Stocker, T.F., D. Qin, G.-K. Plattner, M. Tignor, S.K. Allen, J. Boschung, A. Nauels, Y. Xia, V. Bex and P.M. Midgley (eds.)]. Cambridge University Press,

Cambridge, United Kingdom and New York, NY, USA.

- Jolly, W.M., R. Nemani, and S.W. Running, 2005. A generalized, bioclimatic index to predict foliar phenology in response to climate, *Global Change Biol.*, 11, 619-632.
- Kellner O and Niyogi D., 2014. Assessing drought vulnerability of agricultural production systems in context of the 2012 drought. *J Anim Sci* 92:2811–22.
<https://www.animalsciencepublications.org/publications/jas/pdfs/92/7/2811>
- Knapp, A.K., C.J.W. Carroll, E.M. Denton, K.J. La Pierre, S.L. Collins, and M.D. Smith, 2015. Differential sensitivity to regional-scale drought in six central US grasslands, *Oecologia*, 177 (4), 949-957, doi:10.1007/s00442-015-3233-6.
- Knapp, A. K., and M. D. Smith., 2001. Variation among biomes in temporal dynamics of aboveground primary production. *Science*, 291, 481-484.
- Kunkel, K.E., 2016. update to data originally published in: Kunkel, K.E., D.R. Easterling, K. Hubbard, and K. Redmond. 2004. Temporal variations in frost-free season in the United States: 1895–2000. *Geophys. Res. Lett.* 31:L03201
- Larcher, W., 2003. *Physiological Plant Ecology: Ecophysiology and Stress Physiology of Functional Groups*, 4th ed., Springer, Heidelberg, Germany
- Melillo J.M., T.C.Richmond, G.W.Yohe, 2014: Climate Change Impacts in the United States: The Third National Climate Assessment. U.S. Global Change Research Program. doi:10.7930/J0Z31WJ2
- Moran M.S., G.E. Ponce-Campos, A Huete, M.P. McClaran, Y. Zhang, E. Hamerlynck, D. Augustine, S. Gunter, S. Kitchen, D.P.C. Peters, P.J. Starks and M. Hernandez, 2014. Functional response of US grasslands to the early 21st-century drought. *Ecology* 95:2121–2133
- National Climatic Data Center (NCDC), 2012. NOAA National Centers for Environmental Information, State of the Climate: National Overview for Annual 2011, published online January 2012, retrieved on September 23, 2016 from <http://www.ncdc.noaa.gov/sotc/national/201113>.
- National Climatic Data Center (NCDC), 2013. NOAA National Centers for Environmental Information, State of the Climate: National Overview for Annual 2012, published online January 2013, retrieved on September 23, 2016 from <http://www.ncdc.noaa.gov/sotc/national/201113>.
- Nippert, J.B., Wieme, R.A., Ocheltree, T.W., Craine, J.M., 2012. Root characteristics of C-4 grasses limit reliance on deep soil water in tallgrass prairie. *Plant and Soil* 355 (1–2), 385–394.
- NOAA National Centers for Environmental Information (NCEI), 2016. U.S. Billion-Dollar Weather and Climate Disasters. <https://www.ncdc.noaa.gov/billions/>
- Oak Ridge National Laboratory Distributed Active Archive Center (ORNL DAAC), 2015. FLUXNET Web Page. Available online [<http://fluxnet.ornl.gov>] from ORNL DAAC, Oak Ridge, Tennessee, U.S.A. Accessed May 5, 2015.
- ORNL DAAC, 2008. MODIS Collection 5 Land Products Global Subsetting and Visualization Tool. ORNL DAAC, Oak Ridge, Tennessee, USA. Accessed April 2013. Subset obtained for MOD15A2 and MYD15A2 products at various sites shown in Table 1, time period: 01-01-

2000 to 12-31-2014, and subset size: .25km x .25km: Aggregated to 7km x 7km.
<http://dx.doi.org/10.3334/ORNLDAAAC/1241>

- Parry M.L., O.F. Canziani, J.P. Palutikof, P.J. van der Linden and C.E. Hanson, Eds., 2007. *Climate Change 2007: Impacts, Adaptation and Vulnerability. Contribution of Working Group II to the Fourth Assessment Report of the Intergovernmental Panel on Climate Change*, Cambridge University Press, Cambridge, UK, 982pp. https://www.ipcc.ch/publications_and_data/ar4/wg2/en/ch3s3-4-3.html)
- Pau, S., Edwards, E.J. & Still, C.J., 2013. Improving our understanding of environmental controls on the distribution of C3 and C4 grasses. *Global Change Biology*, 19, 184–196.
- Paruelo JM, Lauenroth WK, 1996. Relative abundance of plant functional types in grasslands and shrublands of North America. *Ecological Applications*, 6, 1212–1224.
- Paruelo, J. M., Lauenroth, W. K., Burke, I. C. & Sala, O. E., 1999. Grassland precipitation–use efficiency varies across a resource gradient. *Ecosystems* 2, 64–68.
- Pereira, A.R., Pruitt, W.O., 2004. Adaptation of the Thornthwaite scheme for estimating daily reference evapotranspiration. *Agric. Water Manage.* 66, 251–257. Popova, Z., Kercheva, M., Pereira, L.S., 20
- PRISM Climate Group, Oregon State University. <http://prism.oregonstate.edu>.
- Raczka BM, Davis KJ, Huntzinger DN et al., 2013. Evaluation of continental carbon cycle simulations with North American flux tower observations. *Ecological Monographs*, 83, 531–556.
- Reichmann, L. G., O. E. Sala, and D. P. C. Peters. 2013. Precipitation legacies in desert-grassland primary production occur through previous-year tiller density. *Ecology* 94:435–443.
- Richardson, A.D., Braswell, B.H., Hollinger, D.Y., Jenkins, J.P., Ollinger, S.V., 2009. Near-surface remote sensing of spatial and temporal variation in canopy phenology. *Ecol. Appl.* 19, 1417–1428.
- Richardson, A. D., et al., 2010. Estimating parameters of a forest ecosystem C model with measurements of stocks and fluxes as joint constraints, *Oecologia*, 164, 25–40, doi:10.1007/s00442-010-1628-y.
- Rienecker, Michele M., and Coauthors, 2011. MERRA: NASA’s Modern-Era Retrospective Analysis for Research and Applications. *J. Climate*, 24, 3624–3648. - See more at: <https://climatedataguide.ucar.edu/climate-data/nasa-merra#sthash.TiZ5KkJt.dpuf>
- Sala, O. E., et al., 2000. Global biodiversity scenarios for the year 2100. *Science*. **287**:1770–1774.
- Schaefer, K., P. Tans, S. Denning, I. Baker, J. Berry, L. Prihodko, N. Suits, and A. Philpott, 2008. The combined Simple Biosphere/Carnegie-Ames-Stanford Approach (SiBCASA) Model, *Jour. Geophys. Res.*, **113**, G03034, doi:10.1029/2007JG000603
- Schaefer, K., et al. 2012. A model-data comparison of gross primary productivity: Results from the North American Carbon Program site synthesis. *Journal of Geophysical Research Biogeosciences* 117:G03010.
- Shafer, M., D. Ojima, J.M. Antle, D. Kluck, R.A. McPherson, S. Petersen, B. Scanlon, and K. Sherman, 2014: *Ch 19: Great Plains. Climate Change Impacts in the United States: The Third National Climate*

- Assessment*, J.M. Melillo, Terese (T.C.) Richmond, and G.W. Yohe, Eds., U.S. Global Change Research Program, 441-461. doi:10.7930/J0D798BC.
- Scheifinger, H., A. Menzel, E. Koch, C. Peter, and R. Ahas, 2002. Atmospheric mechanisms governing the spatial and temporal variability of phenological phases in central Europe, *Int. J. Climatol.*, **22**, 1739–1755
- Schwalm, C. R., et al., 2010. A model-data intercomparison of CO₂ exchange across North America: Results from the North American Carbon Program site synthesis. *Journal of Geophysical Research Biogeosciences* **115**:G00H05.
- Sellers, P. J., D. A. Randall, G. J. Collatz, J. A. Berry, C. B. Field, D. A. Dazlich, C. Zhang, G. D. Collelo, and L. Bounoua, 1996. A revised land surface parameterization of GCMs, Part I: Model formulation, *J. Clim.*, **9**(4), 676
- Still, C.J., Berry, J.A., Collatz, G.J. & DeFries, R.S., 2003. Global distribution of C₃ and C₄ vegetation: carbon cycle implications. *Global Biogeochemical Cycles*, **17**, 1006, doi: 10.1029/2001GB001807
- Stockli, R., T. Rutishauser, P. E. Thornton, L. Lu, and A. S. Denning, 2008. Remote sensing data assimilation for a prognostic phenology model. *Jour. Geophys. Res.* **113**, G04021, doi:10.1029/2008JG000781.
- Stöckli, R., T. Rutishauser, I. Baker, M. A. Liniger, and A. S. Denning, 2011. A global reanalysis of vegetation phenology, *J. Geophys. Res.*, **116**, G03020, doi:10.1029/2010JG001545
- Stocker, T.F., D. Qin, G.-K. Plattner, L.V. Alexander, S.K. Allen, N.L. Bindoff, F.-M. Bréon, J.A. Church, U. Cubasch, S. Emori, P. Forster, P. Friedlingstein, N. Gillett, J.M. Gregory, D.L. Hartmann, E. Jansen, B. Kirtman, R. Knutti, K. Krishna Kumar, P. Lemke, J. Marotzke, V. Masson-Delmotte, G.A. Meehl, I.I. Mokhov, S. Piao, V. Ramaswamy, D. Randall, M. Rhein, M. Rojas, C. Sabine, D. Shindell, L.D. Talley, D.G. Vaughan and S.-P. Xie, 2013: Technical Summary. In: *Climate Change 2013: The Physical Science Basis. Contribution of Working Group I to the Fifth Assessment Report of the Intergovernmental Panel on Climate Change* [Stocker, T.F., D. Qin, G.-K. Plattner, M. Tignor, S.K. Allen, J. Boschung, A. Nauels, Y. Xia, V. Bex and P.M. Midgley (eds.)]. Cambridge University Press, Cambridge, United Kingdom and New York, NY, USA.
- Suttle, K. B., M. A. Thomsen, and M. E. Power., 2007. Species interactions reverse grassland responses to changing climate. *Science*. **315**:640–642.
- Swann, A.L.S, F. Hoffman, C.D. Koven, and J.T. Randerson, 2016. Plant responses to increasing CO₂ reduce estimates of climate impacts on drought severity. *PNAS*. **113** (36) 10019-10024. doi:10.1073/pnas.1604581113
- Taylor, S.H., Hulme, S.P., Rees, M., Ripley, B.S., Ian Woodward, F. & Osborne, C.P., 2010. Ecophysiological traits in C₃ and C₄ grasses: a phylogenetically controlled screening experiment. *New Phytologist*, **185**, 780–791.
- Teeri, J.A. and Stowe, L., 1976. Climatic patterns and distribution of C₄ grasses in North America. *Oecologia*, **23**, 1–12.
- Tieszen LL, B. Reed, N.B. Bliss, B. Wylie, D. DeJong., 1997. NDVI, C₃ and C₄ production, and distributions in Great Plains grassland land cover classes. *Ecological Applications*,

7, 59–78.

“U.S. Drought Monitor Map Archive.” Map Archive. National Drought Mitigation Center (NDMC). University of Nebraska-Lincoln, United States Department of Agriculture, National Oceanic and Atmospheric Administration, 19 Sept. 2016

“U.S. Drought 2012: Farm and Food Impacts.” U.S. Department of Agriculture Economic Research Service (USDA ERS), 26 July 2013. Web 9 Dec. 2015. <http://www.ers.usda.gov/topics/in-the-news/us-drought-2012-farm-and-food-impacts.aspx>.

Vogel, J.C., Fuls, A. & Danin, A., 1986. Geographical and environmental distribution of C-3 and C-4 grasses in the Sinai, Negev, and Judean deserts. *Oecologia*, 70, 258–265.

Walsh, J., D. Wuebbles, K. Hayhoe, J. Kossin, K. Kunkel, G. Stephens, P. Thorne, R. Vose, M. Wehner, J. Willis, D. Anderson, S. Doney, R. Feely, P. Hennon, V. Kharin, T. Knutson, F. Landerer, T. Lenton, J. Kennedy, and R. Somerville, 2014: Ch. 2: Our Changing Climate. *Climate Change Impacts in the United States: The Third National Climate Assessment*, J. M. Melillo, Terese (T.C.) Richmond, and G. W. Yohe, Eds. 2014. U.S. Global Change Research Program, 19-67. doi:10.7930/J0KW5CXT.

Weaver JE, 1968. *Prairie plants and their environment: a fifty-year study in the Midwest*. University of Nebraska Press, Lincoln

White, Michael A., Kirsten M. DE, Beurs, Kamel Didan, 2009. Intercomparison, interpretation, and assessment of spring. *Global Change Biology*. s.l. : Blackwell Publishing Ltd, 2009, pp. 2335-2359

Winslow JC, Hunt ER, Piper SC, 2003. The influence of seasonal water availability on global C3 versus C4 grassland biomass and its implications for climate change research. *Ecological Modelling*, 163, 153–173.